



EDGEWOOD

RESEARCH, DEVELOPMENT & ENGINEERING CENTER

U.S. ARMY CHEMICAL AND BIOLOGICAL DEFENSE COMMAND

ERDEC-CR-219

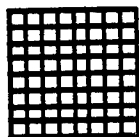
**CATALYTIC OXIDATION OF CYANOGEN CHLORIDE
OVER A MONOLITHIC OXIDATION CATALYST**

**JEFFREY M. CAMPBELL
JOSEPH A. ROSSIN**

**GUILD ASSOCIATES, INC.
Baltimore, MD 21236**

April 1997

Approved for public release; distribution is unlimited.



**Guild
Associates, Inc.**



19970613047

Aberdeen Proving Ground, MD 21010-5423

Disclaimer

The findings in this report are not to be construed as an official Department of the Army position unless so designated by other authorizing documents.

DEPARTMENT OF THE ARMY
U.S. Army Edgewood Research, Development and Engineering Center
Aberdeen Proving Ground, Maryland 21010-5423

ERRATUM SHEET

19 November 1997

REPORT NO. ERDEC-CR-219

TITLE CATALYTIC OXIDATION OF CYANOGEN CHLORIDE
OVER A MONOLITHIC OXIDATION CATALYST

AUTHORS Jeffrey M. Campbell and Joseph A. Rossin

DATE April 1997

CLASSIFICATION UNCLASSIFIED

Please remove the front cover from copies of ERDEC-CR-219 sent to you earlier in 1997 and attach the enclosed replacement cover. Previously printed covers were inadvertently printed with the incorrect activity name and logo.

Sandra J. Johnson

SANDRA J. JOHNSON
Chief, Technical Releases Office

19970613047

AB26101

| REPORT DOCUMENTATION PAGE | | | Form Approved OMB No. 0704-0188 | |
|---|---|---|--------------------------------------|--|
| Public reporting burden for this collection of information is estimated to average 1 hour per response, including the time for reviewing instructions, searching existing data sources, gathering and maintaining the data needed, and completing and reviewing the collection of information. Send comments regarding this burden estimate or any other aspect of this collection of information, including suggestions for reducing this burden, to Washington Headquarters Services, Directorate for Information Operations and Reports, 1215 Jefferson Davis Highway, Suite 1204, Arlington, VA 22202-4302, and to the Office of Management and Budget, Paperwork Reduction Project (0704-0188), Washington, DC 20503. | | | | |
| 1. AGENCY USE ONLY (Leave Blank) | 2. REPORT DATE 1997 April | 3. REPORT TYPE AND DATES COVERED Final; 94 Sep - 95 May | | |
| 4. TITLE AND SUBTITLE Catalytic Oxidation of Cyanogen Chloride Over a Monolithic Oxidation Catalyst | | 5. FUNDING NUMBERS C-DAAA15-93-C-0070 | | |
| 6. AUTHOR(S) Campbell, Jeffrey M., and Rossin, Joseph A. | | | | |
| 7. PERFORMING ORGANIZATION NAME(S) AND ADDRESS(ES) Guild Associates, Inc., 5022 Campbell Boulevard, Baltimore, MD 21236 | | 8. PERFORMING ORGANIZATION REPORT NUMBER ERDEC-CR-219 | | |
| 9. SPONSORING/MONITORING AGENCY NAME(S) AND ADDRESS(ES) | | 10. SPONSORING/MONITORING AGENCY REPORT NUMBER | | |
| 11. SUPPLEMENTARY NOTES COR.: David H. Reed, SCBRD-RT/ASM, (410) 671-8212 | | | | |
| 12a. DISTRIBUTION/AVAILABILITY STATEMENT Approved for public release; distribution is unlimited. | | 12b. DISTRIBUTION CODE | | |
| 13. ABSTRACT (Maximum 200 words) The catalytic oxidation of cyanogen chloride was evaluated over a monolithic oxidation catalyst at temperatures between 200 and 300 °C in air employing feed concentrations between 100 and 10,000 ppm (274 and 27,400 mg/m ³). Water was found to have an effect on the performance of the catalyst. In the absence of water, the catalytic activity was very low. Increasing the concentration of water to slightly >0.25 %, significantly increased the catalytic activity. Isothermal reaction rate data were measured by exposing the catalyst to various concentrations of cyanogen chloride and recording the conversion of cyanogen chloride as a function of residence time. Reaction rate data were correlated using a mathematical model, which took into account external mass transfer resistances and kinetic effects, and included terms to account for inhibition due to adsorption of reactant and product HCl onto adsorption sites. In humid air, no deactivation of the catalyst was observed. In dry air, the catalyst rapidly deactivated. However, the initial activity could be restored upon adding water to the feed stream. Reaction products for the oxidation of cyanogen chloride in humid air consisted of CO ₂ , HCl, N ₂ , N ₂ O, and NO _x , with the NO _x selectivity being greatest at high reaction temperature. | | | | |
| 14. SUBJECT TERMS Cyanogen chloride Catalytic oxidation Catalysis | | | 15. NUMBER OF PAGES 40 | |
| | | | 16. PRICE CODE | |
| 17. SECURITY CLASSIFICATION OF REPORT UNCLASSIFIED | 18. SECURITY CLASSIFICATION OF THIS PAGE UNCLASSIFIED | 19. SECURITY CLASSIFICATION OF ABSTRACT UNCLASSIFIED | 20. LIMITATION OF ABSTRACT UL | |

Blank

PREFACE

The work described in this report was performed under Contract No. DAAA15-93-C-0070, Design and Development of Regenerable Air Filtration Units and Integration into Host Applications. This work was started in September 1994 and completed in May 1995.

The use of either trade or manufacturers' names in this report does not constitute an official endorsement of any commercial products. This report may not be cited for purposes of advertisement.

This report has been approved for public release. Registered users should request additional copies from the Defense Technical Information Center; unregistered users should direct such requests to the National Technical Information Service.

DTIC QUALITY INSPECTED 3

Blank

CONTENTS

| | | |
|----|---|----|
| 1. | INTRODUCTION..... | 7 |
| 2. | EXPERIMENTAL METHODS..... | 8 |
| 3. | MODEL DEVELOPMENT AND FIT PARAMETER ESTIMATION..... | 13 |
| 4. | RESULTS AND DISCUSSION..... | 15 |
| 5. | CONCLUSIONS..... | 24 |
| | LITERATURE CITED..... | 27 |
| | Appendix : FORTRAN routine used to determine kinetic fit parameters.. | 29 |

FIGURES

| | |
|--|----|
| Figure 1: Schematic Representation of Fixed Bed Catalytic Reactor System..... | 9 |
| Figure 2: Sample GC trace showing feed and effluent analysis..... | 12 |
| Figure 3: Schematic Representation of a Monolith Channel..... | 13 |
| Figure 4: Axial temperature deviation recorded during the oxidation of cyanogen chloride at 300°C..... | 16 |
| Figure 5: Conversion as a function of temperature for the oxidation of 1,000 ppm cyanogen chloride in air as a function of water concentration..... | 17 |
| Figure 6: Nitrogen-product concentration (A) and nitrogen-product selectivity (B) as a function of reaction temperature for the oxidation of 1,000 ppm cyanogen chloride in humid air..... | 18 |
| Figure 7: Conversion as a function of time-on-stream for the oxidation of 1,000 ppm cyanogen chloride in humid air at 275°C..... | 19 |
| Figure 8: Conversion as a function of time-on-stream for the oxidation of 1,000 ppm cyanogen chloride in dry air at 400°C..... | 20 |
| Figure 9: Conversion of cyanogen chloride as a function of residence time in humid air at 200°C..... | 22 |
| Figure 10: Conversion of cyanogen chloride as a function of residence time in humid air at 250°C..... | 22 |
| Figure 11: Conversion of cyanogen chloride as a function of residence time in humid air at 275°C..... | 23 |
| Figure 12: Conversion of cyanogen chloride as a function of residence time in humid air at 300°C..... | 23 |
| Figure 13: Parity plot of predicted versus experimental conversion of cyanogen chloride..... | 24 |
| Figure 14: Reduction ratio, C_a / C_a^0 , of cyanogen chloride as a function of residence time at 300°C..... | 25 |

CATALYTIC OXIDATION OF CYANOGEN CHLORIDE OVER A MONOLITHIC OXIDATION CATALYST

1. INTRODUCTION

Present air purification systems designed for removal of chemical warfare agents from air streams are based solely on activated, impregnated carbon, namely ASC whetlerite. While these filters function well against a wide range of chemical agents, they possess several shortcomings. First, the carbon filter has a limited capacity for agents which are removed by chemical reaction and those which are weakly adsorbed. Second, prolonged environmental exposure has been shown to reduce the capacity of these filters for agents which are removed by chemical reaction¹. The result of these shortcomings is to impose change-out requirements which may present logistical as well as disposal burdens to the user. Catalytic oxidation is an alternative air purification technology which is being investigated as a means of alleviating the above mentioned burdens.

Catalytic oxidation has been proven to be a viable means of controlling industrial offgas emissions^{2,3}. Offgas streams containing chlorinated organic molecules present an additional concern in that the chlorine associated with these compounds has the potential to poison/inhibit the catalyst^{2,4-9}. Studies by Rossin et al.^{4,8,9} report that the oxidation of chlorine-containing compounds over supported platinum catalysts will be significantly inhibited due to the adsorption of product HCl onto catalytic sites. The observed inhibition is, however, reversible. Deactivation resulting from the oxidation of chlorine-containing compounds has been observed by several investigators^{2,4-9}. For example, Rossin and Farris⁸ report a decrease in the conversion of 1,500 ppm chloroform over a 2% Pt/ α -Al₂O₃ catalyst from 92 to 83% over the duration of a 65 hour experiment. Lester¹⁰, however, claims that a titania based catalyst is capable of oxidizing chlorine-containing compounds without deactivation.

The catalytic oxidation of nitrogen-containing compounds has the potential to form NO_x¹¹⁻¹³. Lester and Homeyer¹¹ studied the destruction of a number of amines over a monolithic catalyst which presumably contained platinum. In all cases, the NO_x selectivity was significant, especially at high reaction temperatures. Rossin¹², in a study involving the oxidation of hydrogen cyanide over a platinum monolith, reported that while the catalyst could readily destroy hydrogen cyanide, NO_x selectivities were unacceptable. Later, Rossin and Campbell¹³ reported a catalytic process for direct oxidation of nitrogen-containing compounds without the formation of NO_x. The catalyst employed by the process, whose details were not disclosed, represents a significant advantage in selectivity over conventional oxidation catalysts.

The objective of this study was to develop an experimentally based reactor design equation which would be capable of describing the oxidation of cyanogen chloride over a wide range of process conditions. The approach taken in meeting this objective was to first record isothermal reactor design data over a wide range of temperatures,

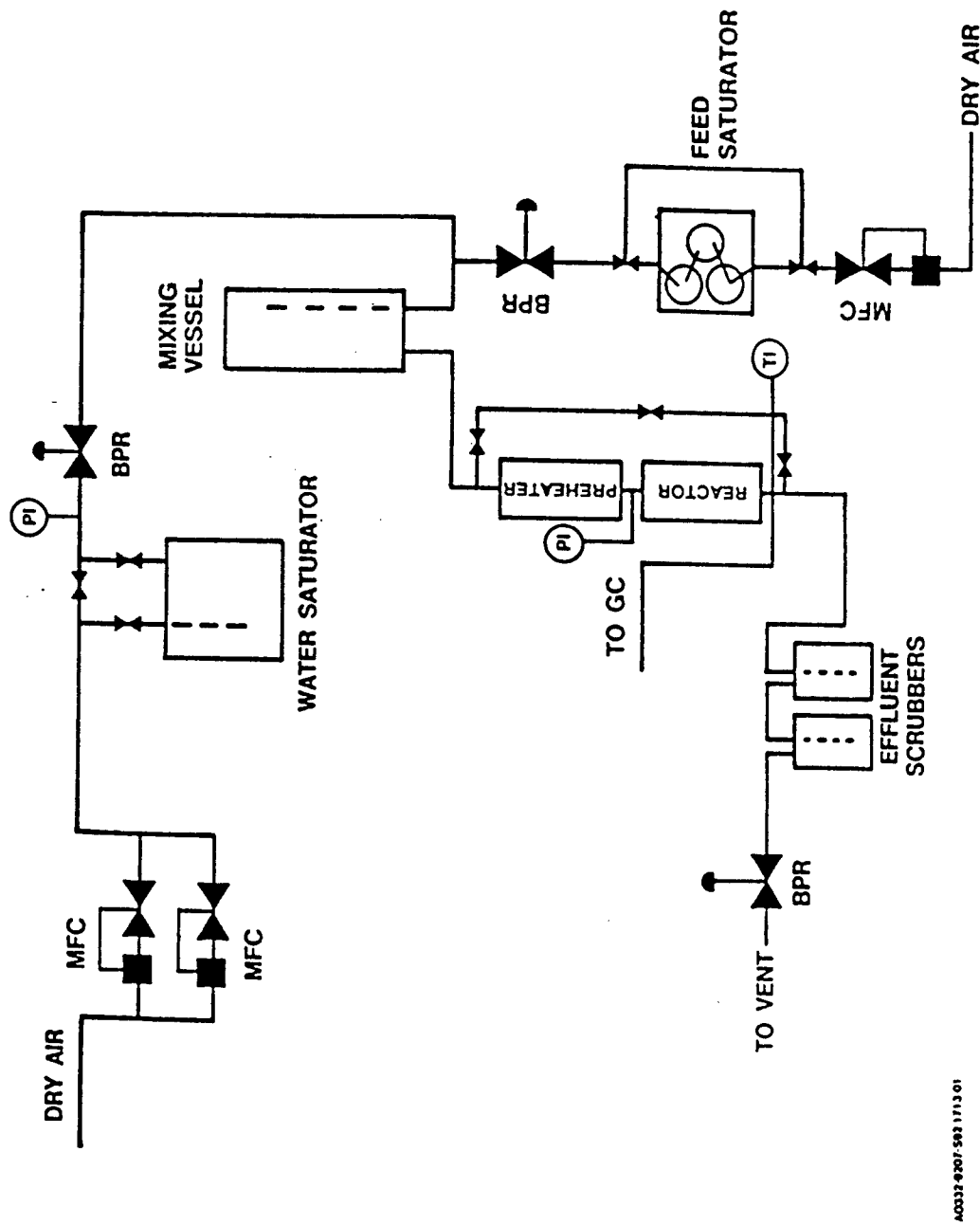
concentrations and residence times, and then correlate the design data using a reactor design equation which takes into account all necessary transport resistances and kinetic effects. Also included in this effort was quantitatively identifying all reaction products formed during the oxidation of cyanogen chloride, assessing the effects of water on catalyst performance, and assessing the significance of catalyst deactivation.

2. EXPERIMENTAL METHODS

Materials: Cyanogen chloride was obtained from Aberdeen Proving Ground. Analysis revealed the compound to be greater than 99% pure. Neat cyanogen chloride was metered into a 17 liter pressure vessel and diluted with either air or helium such that the concentration of cyanogen chloride in the vessel was 1.0% by volume. Calibration gases (namely CO, CO₂, NO and NO₂) were obtained from Matheson. The catalyst employed during this study was the Military Air Purification (MAP) catalyst and was obtained from Allied Signal. The catalyst was a platinum monolith with a cell density of 93 cells/cm².

Catalyst Preparation: Catalyst cores were cut from a 30 cm diameter by 10.2 cm long monolith block using a diamond tip hole saw. The catalyst was a ceramic monolith possessing 93 channels per cm². Once cut, the resulting catalyst core was approximately 2.2 cm diameter by 6.0 cm long. The center channels of the monolith were plugged with alundum cement so that only the channels near the outer circumference of the catalyst core (totaling 115 channels) remained open. The resulting catalyst volume was 7.42 cm³. Preparing the catalyst in this manner minimizes axial and radial temperature gradients, thereby allowing one to record reaction rate data under near isothermal conditions^{12,14}. Following preparation, the catalyst core was wrapped with a thin layer of glass wool and loaded into the reactor. The glass wool was used to maintain a seal between the catalyst and the reactor wall, thereby preventing the gas stream from by-passing the catalyst. Once loaded into the reactor, seven type K fine-wire thermocouples were extended axially into unobstructed channels of the monolith. These thermocouples were located 0.5 cm above the monolith, and 0.5, 1.0, 2.0, 3.0, 4.0 and 5.0 cm from the inlet, and were used to assess the axial temperature gradient within the monolith.

Equipment: A schematic representation of the fixed bed reactor system is illustrated in Figure 1. Dry, oil-free air from a PSA air drier was metered to the reactor using either a 0-5 or 0-20 NL/min mass flow controller. NL is defined as one liter of dry air at 0°C and one atmosphere pressure. Dry air from the mass flow controller was then delivered to a water saturator, which was housed in a temperature controlled chamber. A back pressure regulator is located downstream of the water saturator. The concentration of water in the air stream may be controlled by controlling the temperature and pressure of the water saturator. In addition, the water saturator could be by-passed to conduct the experiments in dry air.



AO332-9207-582 1/13 01

Figure 1: Schematic representation of fixed bed catalytic reactor system. BPR: back pressure regulator; GC: gas chromatograph; MFC: mass flow controller.

Cyanogen chloride was delivered to the air stream from a compressed gas cylinder containing approximately 4.0% cyanogen chloride in helium. The reactant stream was metered into the humidified air stream via one of three mass flow controllers; 0-50 Nml/min, 0-200 Nml/min and 0-2,000 Nml/min. Nml refers to normal milliliter and is defined as one liter of air at 0°C, one atmosphere pressure. In some cases, the 0-2,000 Nml/min flow controller was replaced with a 0-5,000 Nml/min controller. Use of this flow controller bank allowed for achieving a wide range of cyanogen chloride concentrations over the desired air flow rate range.

Once blended, the feed stream was delivered to the catalytic reactor. The reactor consisted of a 66 cm long glass tube approximately 2.5 cm in diameter. The upper 40 cm of the glass reactor served as the pre-heat zone and was filled with 4 mm diameter glass beads. The glass beads provided further mixing of the feed gas as well as surface area for heating the incoming feed stream to reactor temperature. The reactor tube was housed in an 8.9 cm diameter by 60 cm long aluminum block. The aluminum block was electrically heated, and the temperature of the reactor was controlled by controlling the temperature of the aluminum block. The catalyst core was located approximately 7 to 10 cm below the pre-heat zone of the reactor.

Following the reactor, the effluent stream was delivered to a catalytic filter, which was designed to destroy any unreacted cyanogen chloride in the effluent stream. Following the catalytic filter, the air stream was delivered to two scrubber tanks in series. Each scrubber tank was filled approximately half way with a 10 molar sodium hydroxide solution and served to remove hydrochloric acid (a reaction product) from the effluent stream. Flow from the scrubber vessels was delivered to a back pressure regulator, which served to maintain a constant pressure on the reactor. Following the back pressure regulator, the air stream was vented into a fume hood. All lines in contact with cyanogen chloride were contained within the fume hood and were electrically heat traced.

Isothermal Reaction Rate Measurements: Reaction rate data were recorded at temperatures of 200, 250, 275 and 300°C at a pressure of 6 ± 1 psig. The feed concentration of cyanogen chloride was varied between 100 and 10,000 ppm (274 and 27,400 mg/m³)¹ in humid ($T_{\text{dew}} = 23 \pm 1^\circ\text{C}$) air. The residence time, based on the reactor volume occupied by the unobstructed monolith channels and calculated at 0°C and 1 atm pressure, was adjusted in an effort to achieve conversions between 10 and 95%. Air flow rates were typically varied between 2 and 25 NL/min. Reaction rate data were recorded only during day-time hours. Overnight, the catalyst was maintained at reaction temperature under flowing, humid air. The same catalyst core was used for all experiments conducted in this study. All process conditions were maintained for between 1 to 3 hours to ensure the achievement of steady-state. It should be noted that for feed concentrations greater than about 1,000 ppm, an increase in the catalyst temperature was observed. In these instances, the catalyst temperature was adjusted such that the average catalyst temperature (numerical average based on the thermocouple measurements) was $\pm 2^\circ\text{C}$ of the desired value. Both feed and effluent streams were analyzed continuously for

¹ Concentrations reported in mg/m³ are referenced to 0°C, one atmosphere pressure.

CO₂ and cyanogen chloride during all runs. The conversion of cyanogen chloride was determined based on the concentration of cyanogen chloride in the feed and effluent streams.

Effects of Water: The effects of water concentration on the catalytic activity were determined by recording the conversion of cyanogen chloride as a function of reaction temperature for water concentrations of <0.03%, 0.1%, 0.25%, 0.60%, 1.14% and 2.71%. These concentrations correspond to dew point temperatures of <-35°C, -22°C, -11°C, 0°C, 10°C and 23°C, respectively, at one atmosphere pressure. The dew point temperature of <-35°C corresponds to air delivered from the PSA air drier. The run was initiated by heating the reactor to 320°C in flowing, humid air at a residence time of 0.25 seconds. Once at temperature, cyanogen chloride was introduced to the feed stream at a rate required to achieve a concentration of 1,000 ppm. These process conditions were maintained for approximately one hour, at which time, the catalyst temperature was decreased to 170°C at 30°C/hr, with the effluent stream sampled every 20 minutes (10°C temperature intervals) for CO₂, N₂O and cyanogen chloride in the feed and effluent stream. For the run conducted with a dew point temperature of <-35, the run was initiated by heating the reactor to 400°C.

Catalyst stability: The stability of the catalyst was evaluated by exposing it to 1,000 ppm cyanogen chloride in humid ($T_{\text{dew}} = 23 \pm \text{C}$) air employing a residence time of 0.05 seconds at 275°C. These process conditions were maintained for 68 hours, at which time the run was terminated. During the run, the effluent stream was sampled for the concentration of CO₂, N₂O and cyanogen chloride every hour. Just prior to termination of the run, the effluent stream was sampled for the concentration of HCl and Cl₂ using Dräger tubes.

Upon termination of the run, an additional test was performed in dry air ($T_{\text{dew}} < -35^\circ\text{C}$) employing a residence time of 0.50 seconds and a cyanogen chloride feed concentration of 1,000 ppm. This run was conducted at 400°C. Prior to the start of the run, the catalyst was exposed to the dry air stream overnight in order to remove all traces of water from the lines as well as equilibrate the catalyst with respect to the concentration of hydroxyls on the surface. The run was then initiated the next morning and discontinued following 8 hours of operation. Upon termination of the run, the catalyst was cooled to 275°C, and the previously conducted stability run was performed.

Sample Analysis: During the reaction rate studies, the concentration of cyanogen chloride in the feed and effluent stream, and the concentration of CO₂ and N₂O in the effluent stream were monitored using a gas chromatograph. All analyses were performed using a Hewlett-Packard 5890 gas chromatograph (GC) equipped with both a flame ionization detector (FID) and a thermal conductivity detector (TCD) and automatic sampling valves. A sample of the GC trace is reported in Figure 2. Cyanogen chloride was analyzed using a 2 m by 3.2 mm diameter Hayesep Q column attached to the FID, while CO₂ and N₂O were analyzed using a 2 m by 3.2 mm diameter Hayesep Q column attached to the TCD. Samples were analyzed first by sampling the effluent for CO₂ and

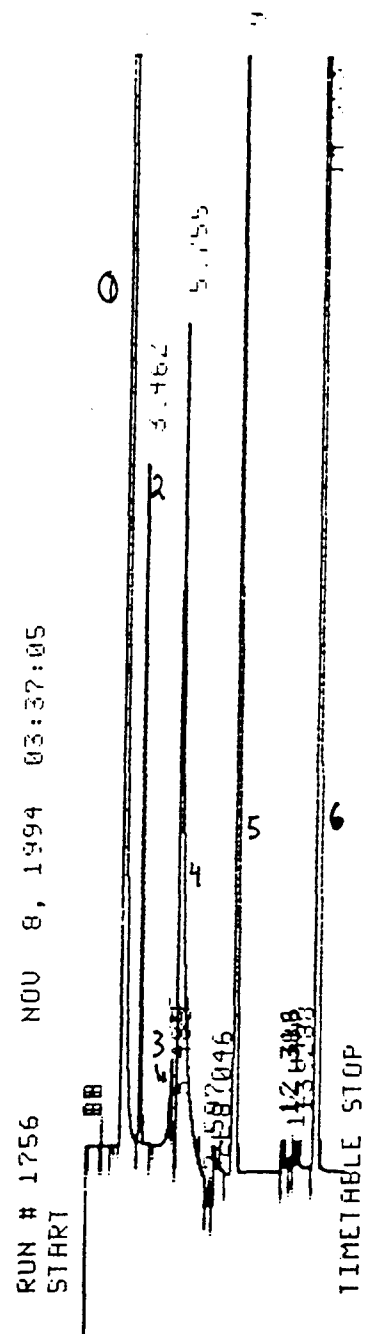


Figure 2: Sample GC trace showing feed and effluent analysis. 1. Air, 2. CO₂, 3. N₂O, 4. H₂O, 5. Cyanogen Chloride (effluent), 6. Cyanogen Chloride (feed).

N₂O at 60°C, then heating the oven to 120°C at 40°C/min and sampling the effluent for cyanogen chloride. Following this, the feed stream was sampled for cyanogen chloride. The above analysis sequence required 17 minutes to perform.

3. MODEL DEVELOPMENT AND FIT PARAMETER ESTIMATION

Reaction Rate Model Development: The monolithic oxidation catalyst employed in this study consisted of a series of straight, parallel channels. The monolith substrate is coated with a thin layer of catalyst support material, termed washcoat. The catalytic metals are impregnated onto the washcoat. The monolith employed in this study had square channels, with a channel density 93 cells/cm². The thickness of the washcoat and substrate were not supplied by the manufacturer. For modeling purposes, the washcoat was assumed to be 0.0035 cm thick, and the substrate was assumed to be 0.0115 cm thick. A schematic representation of a monolith channel is provided below in Figure 3. Based on these dimensions, the monolith is 11.55% washcoat plus catalyst.

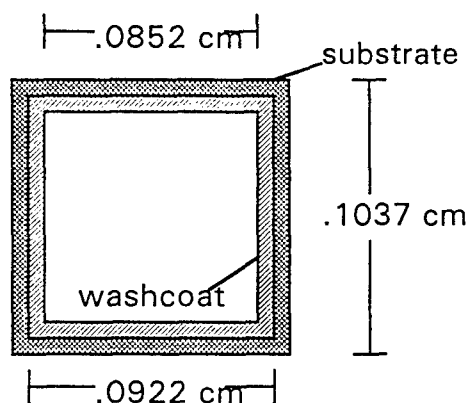


Figure 3: Schematic Representation of a Monolith Channel.

The oxidation of cyanogen chloride was modeled according to the reaction rate expression:

$$\text{Rate} = \frac{AC_{CK}}{1 + BC_{HCl} + DC_{CK}} \quad (1)$$

In the above reaction rate expression, A, B and D are fit parameters (s⁻¹, cm³/mol and cm³/mol, respectively), C_{HCl} is the concentration of hydrochloric acid (mols/cm³), C_{CK} is the concentration of cyanogen chloride (mols/cm³) and Rate is the reaction rate (mols/s-cm³ catalyst). The reaction rate expression may be derived by assuming the reaction occurs via adsorption of cyanogen chloride onto surface hydroxyls followed by decomposition of the adsorbed species. The concentration of oxygen was held constant during all experiments (21%) and was in great excess (meaning that regardless of the cyanogen chloride conversion, the concentration of oxygen did not change significantly over the length of the reactor). Therefore, the concentration of oxygen was not taken into account. The rate expression also does not take into account the concentration of water.

As long as the concentration of water was greater than the concentration of cyanogen chloride, the concentration of water did not affect the reaction rate.

The above rate expression was incorporated into a fixed bed reactor design equation which took into account external mass transfer resistances and kinetic effects. The equations which govern mass transfer and chemical reaction rates within the channel of the monolith are¹⁵:

$$\bar{v} \frac{dC_{CK}^g}{dz} = k_m A [C_{CK}^s + C_{CK}^g] \quad (2)$$

$$\text{Rate} = k_m A' [C_{CK}^g - C_{CK}^s] \quad (3)$$

where \bar{v} is the average linear velocity within the channel at reaction conditions (cm/s), C_{CK}^g and C_{CK}^s refer to the gas and solid phase concentration of cyanogen chloride, respectively, calculated at reaction conditions (mols/cm³), dz is the differential reactor length (cm), k_m is the mass transfer coefficient (cm/s), A is the surface area of the monolith channel (cm²/cm³ void), Rate is the reaction rate as defined by eq. 1 (mols/s-cm³-cat), and A' is the surface area of the catalyst (cm²/cm³ catalyst). The above reaction rate expressions were numerically integrated using a multistep method. Data were correlated over the entire data set simultaneously, rather than by the standard technique of determining the fit parameters at each reaction temperature, followed by correlating the data using Arrhenius type equations. Therefore, both the activation energy/heats of adsorption and pre-exponential factors were determined simultaneously. The algorithm used to determine the fit parameters employed numerical derivatives and minimized the error between the predicted and experimental conversions. The mass transfer coefficient was determined from a limiting Sherwood number correlation¹⁵⁻¹⁶:

$$\text{Sh} = 3.66(1 + 0.95 \text{ReSc} \frac{d}{z})^{0.45} \quad (4)$$

$$k_m = \frac{\text{Sh} D_{ab}}{2R_h} \quad (5)$$

where Sh is the Sherwood number, Re is the Reynolds number, Sc is the Schmidt number, d is channel diameter (cm), D_{ab} is the diffusion coefficient for cyanogen chloride in air (cm²/s), and R_h is the hydraulic radius of the channel (cm). The diffusion coefficient was estimated to be 0.067 cm²/s at 0°C and was allowed to increase proportional to temperature to the power of 1.5 ($T^{1.5}$). Using the reactor design equations, the fit parameters were determined to be:

$$\begin{aligned} A &= 1.8631(08) \exp(-6,075/T) \text{ s}^{-1} \\ B &= 1.9446(04) \exp(+4,456/T) \text{ cm}^3/\text{mol} \\ D &= 3.0643(05) \exp(+2,695/T) \text{ cm}^3/\text{mol} \end{aligned}$$

4. RESULTS AND DISCUSSION

Axial Temperature Deviation: Oxidation reactions are highly exothermic. When recording reaction rate data, it is desired to minimize heat transfer effects so that near isothermal operation of the catalyst is achieved. In this manner, kinetic effects will not be masked by heat transfer effects. For pelleted and granular catalysts, temperature excursions in the laboratory reactor can be and often are controlled by diluting the catalyst bed with inert particles of a similar mesh size. The monolithic oxidation catalyst consists of a single piece of substrate and thus cannot be diluted in the same manner as granular catalysts are. Therefore, recording reaction rates under near isothermal conditions presents a challenge to the investigator.

A differential mode of operation presents one option for minimizing the axial temperature gradients. Stock and Lowe^{17,18} have measured quality reaction rate data for the oxidation of carbon monoxide by operating the monolith under differential conditions. However, a differential mode of operation was felt to be inappropriate for the present study. This is because the low residence times required to maintain differential conditions may result in entrance and exit effects dominating the fluid dynamics within the monolith channel, rather than the laminar flow that would be encountered by the application. Also, reaction rate inhibition due to the adsorption of reaction products onto catalytically reactive sites, as has been reported previously for the oxidation of chlorine-containing compounds^{8,9}, may be difficult to assess, since the concentration of the reaction products will be minimal. Reaction products could always be added to the feed stream, but this would only add an additional order of complexity to an already complex problem.

The oxidation of cyanogen chloride in air is highly exothermic. The heat of reaction (at 298 K) was estimated to be 107.9 kcal/mol. The adiabatic temperature rise (corresponding to 100% destruction of CK) for cyanogen chloride concentrations of 1,000, 3,000 and 10,000 ppm were calculated to be 13.8, 41.4 and 138°C, respectively. Because of the heat generated by the reaction, one can anticipate difficulties in maintaining a uniform temperature along the catalyst length, especially as the concentration of reactant and reaction temperature are increased. The technique to minimize the axial temperature gradient, as described in the Experimental Methods section, involved limiting the heat generated within the volume of reactor occupied by the monolith core by obstructing the center channels of the monolith. Therefore, the reaction would only proceed in channels located near the reactor wall, and the ratio of the heat generated to surface area of the reactor tube is maximized.

Figure 4 reports the temperature deviation for the oxidation of cyanogen chloride at 300°C. Temperature deviation refers to the difference between the catalyst temperature recorded at discrete points within the monolith and the average of the temperature measurements. Data correspond to cyanogen chloride feed concentrations of 1,000, 3,000 and 10,000 ppm (2,740, 8,220 and 27,400 mg/m³) and were recorded under conditions where the conversion of cyanogen chloride was greater than 90%. As expected, the temperature uniformity of the catalyst was greatly improved at lower conversions and at

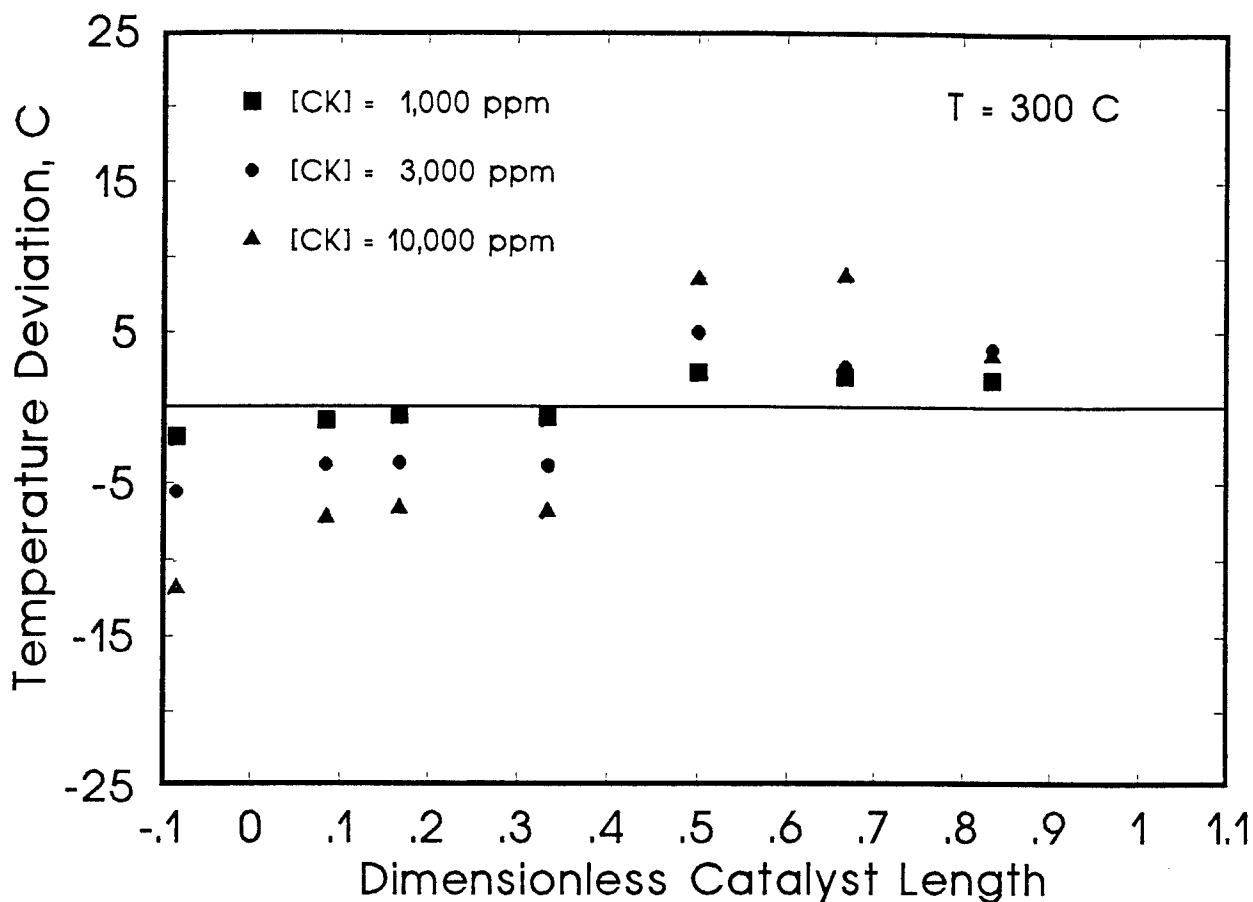


Figure 4: Axial temperature deviation recorded during the oxidation of cyanogen chloride at 300°C.

lower reaction temperatures. For feed concentrations of 3,000 ppm (8,220 mg/m³) and below, the axial temperature deviation was typically less than $\pm 5^\circ\text{C}$. For feed concentrations of 10,000 ppm (27,400 mg/m³), the axial temperature deviation increased to almost $\pm 10^\circ\text{C}$. These results attest to the near isothermal operation achieved via modification of the monolith core.

Effects of Water: Figure 5 reports conversion as a function of temperature for the oxidation of 1,000 ppm (2,740 mg/m³) cyanogen chloride in air with different concentrations of water. Data reported in this figure were recorded at a residence time of 0.25 s. Results presented in this figure show that increasing the concentration of water from 0 to 0.25% ($T_{\text{dew}} = -35$ and -11°C) has a significant effect on the conversion of cyanogen chloride; however, further increasing the concentration of water to 2.7% ($T_{\text{dew}} = 23^\circ\text{C}$) did not affect the conversion of cyanogen chloride. These results can be explained assuming the reaction is initiated by the hydrolysis of cyanogen chloride, rather than by an oxidative mechanism. A hydrolysis reaction involving cyanogen chloride would proceed via an interaction between a cyanogen chloride molecule and a hydroxyl group on the surface of the catalyst to form (possibly) an adsorbed -OCN species plus hydrochloric acid. The -OCN species may then decompose to form the reaction products.

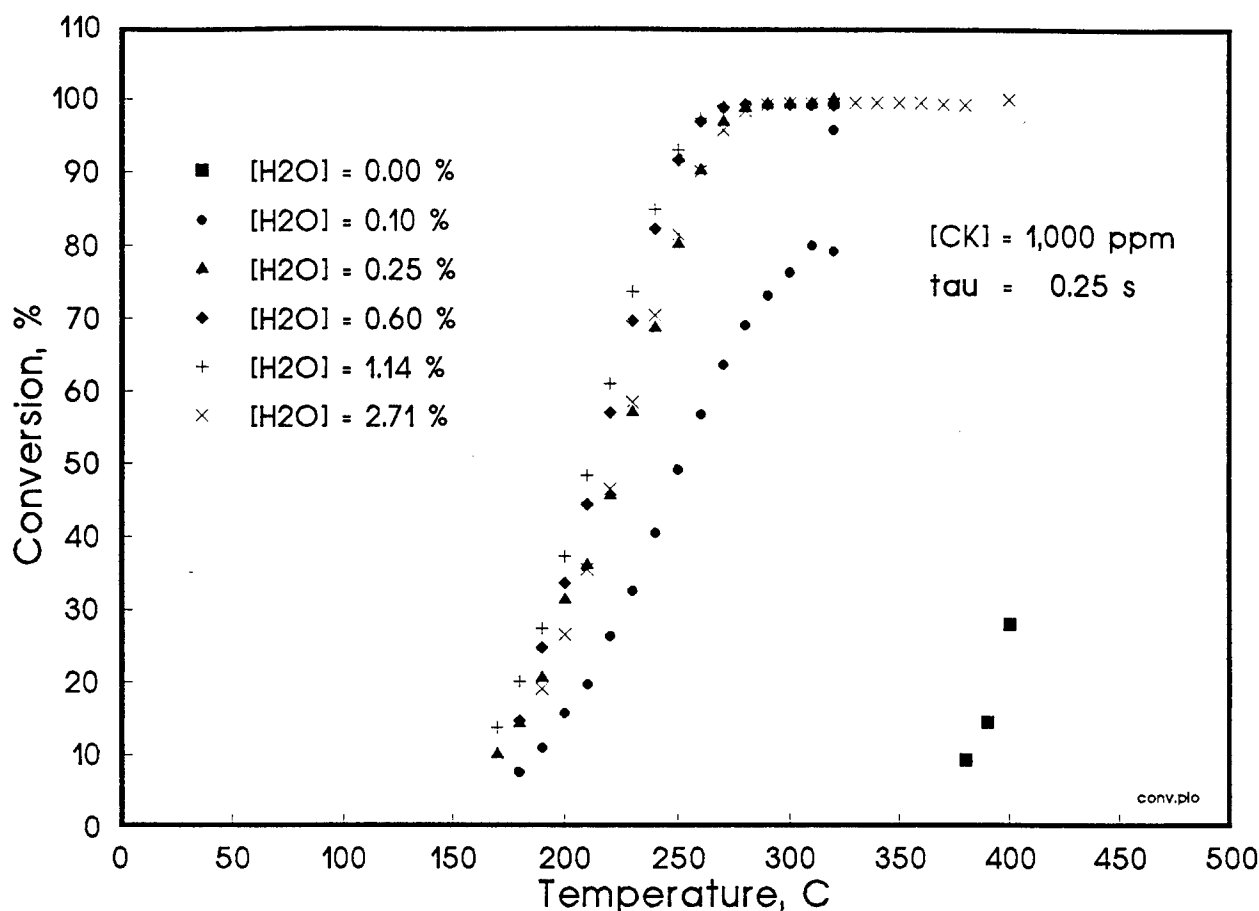


Figure 5: Conversion as a function of temperature for the oxidation of 1,000 ppm cyanogen chloride in air as a function of water concentration.

One possible explanation for the effects of water on the catalyst performance stems from the chemisorption of water on the surface of the catalyst. At low water concentrations, the surface of the catalyst is not saturated with hydroxyls; i.e. there are sites available for adsorption of water. Under these conditions, increasing the concentration of water in the feed stream will increase the hydroxyl concentration at the surface of the catalyst, thereby increasing the catalytic activity. Upon further increasing the concentration of water in the feed stream, the catalyst surface becomes saturated with hydroxyls; i.e. there are no more sites available for water adsorption. As a result, the reaction rate is no longer a function of the concentration of water in the feed stream.

Reaction Products: The only carbon-containing reaction product identified in the reactor effluent stream was carbon dioxide. No carbon monoxide or products of partial oxidation were identified. Carbon balances were typically $100 \pm 5\%$ for all runs conducted in this study. Figure 6 reports the product distribution of the nitrogen-containing reaction products as a function of temperature for the oxidation of 1,000 ppm cyanogen chloride at atmospheric pressure. This test was conducted by placing a small piece of monolith into a 0.95 cm o.d. glass tube and performing the test in the micro-reactor system. In this

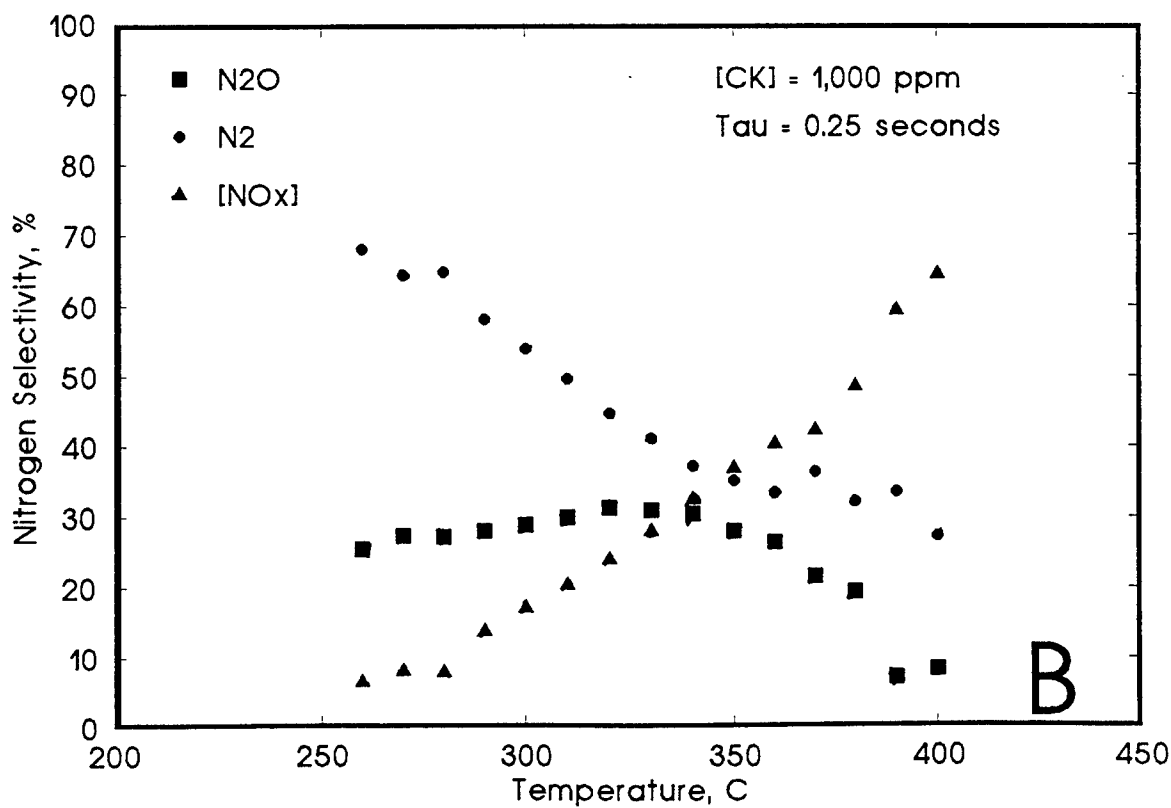
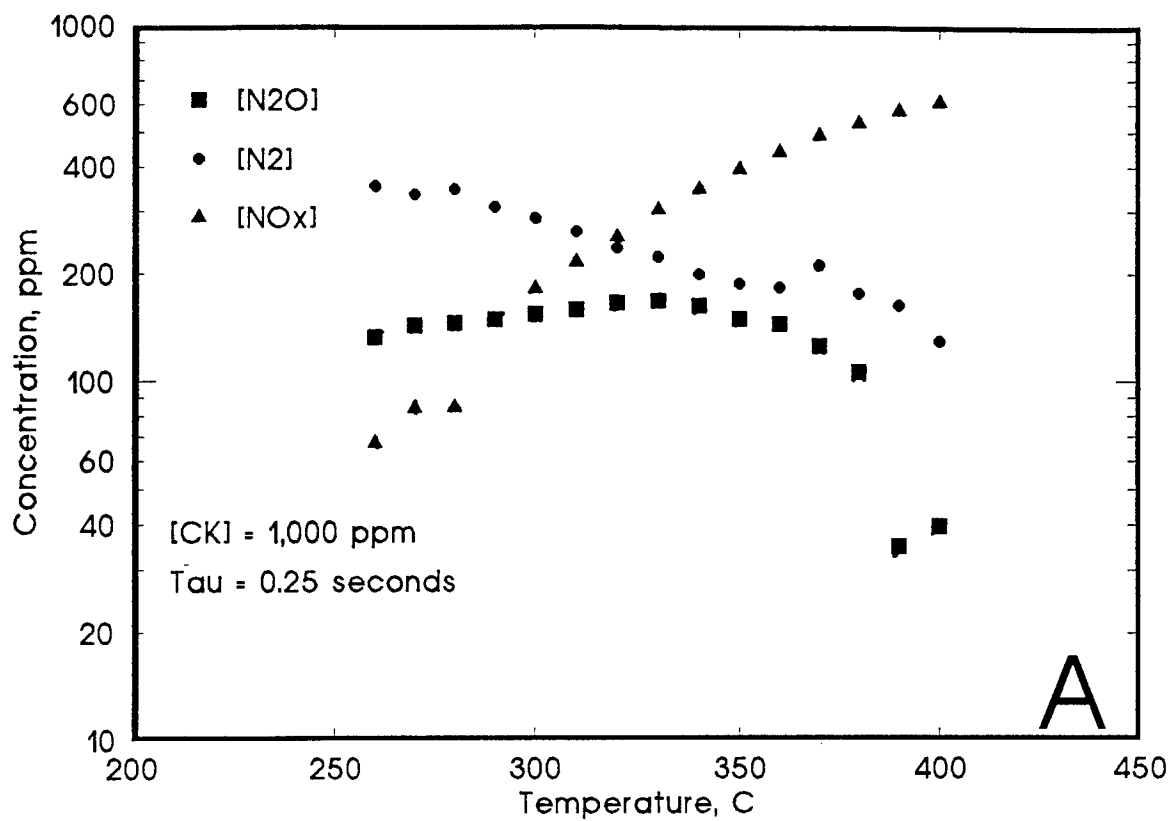


Figure 6: Nitrogen-product concentration (A) and nitrogen-product selectivity (B) as a function of reaction temperature for the oxidation of 1,000 ppm cyanogen chloride in humid air.

manner, near isothermal operation could be achieved and the product distribution would not be skewed as a result of temperature effects. Nitrogen-containing reaction products consisted of N_2 , N_2O , NO and NO_2 , with NO plus NO_2 being collectively referred to as NO_x in Figure 6. The product distribution was found to vary as a function of temperature, with the formation of NO_x favored at high temperatures, and the formation of the reduced products (N_2 and N_2O) favored at the lower temperatures. At 400°C , approximately 65% of the nitrogen-containing products (on an atomic nitrogen basis) consist of NO_x . Below 300°C , NO_x decreases to less than 15%; however, under no conditions where the cyanogen chloride conversion was greater than 99% was NO_x not measured in the effluent stream. Results presented in Figure 6 are important because NO_x will be difficult to remove from a reactor effluent stream. Campbell and Rossin (1995) reported a catalyst capable of destroying nitrogen-containing compounds without the formation of NO_x . Such a catalyst would be required to meet the demands associated military chemical defense applications.

Catalytic Deactivation: Figure 7 reports the conversion of 1,000 ppm (2,740 mg/m^3) cyanogen chloride as a function of time-on-stream in humid air. Data were recorded at 275°C employing a residence time of 0.05 seconds. Results illustrate that the

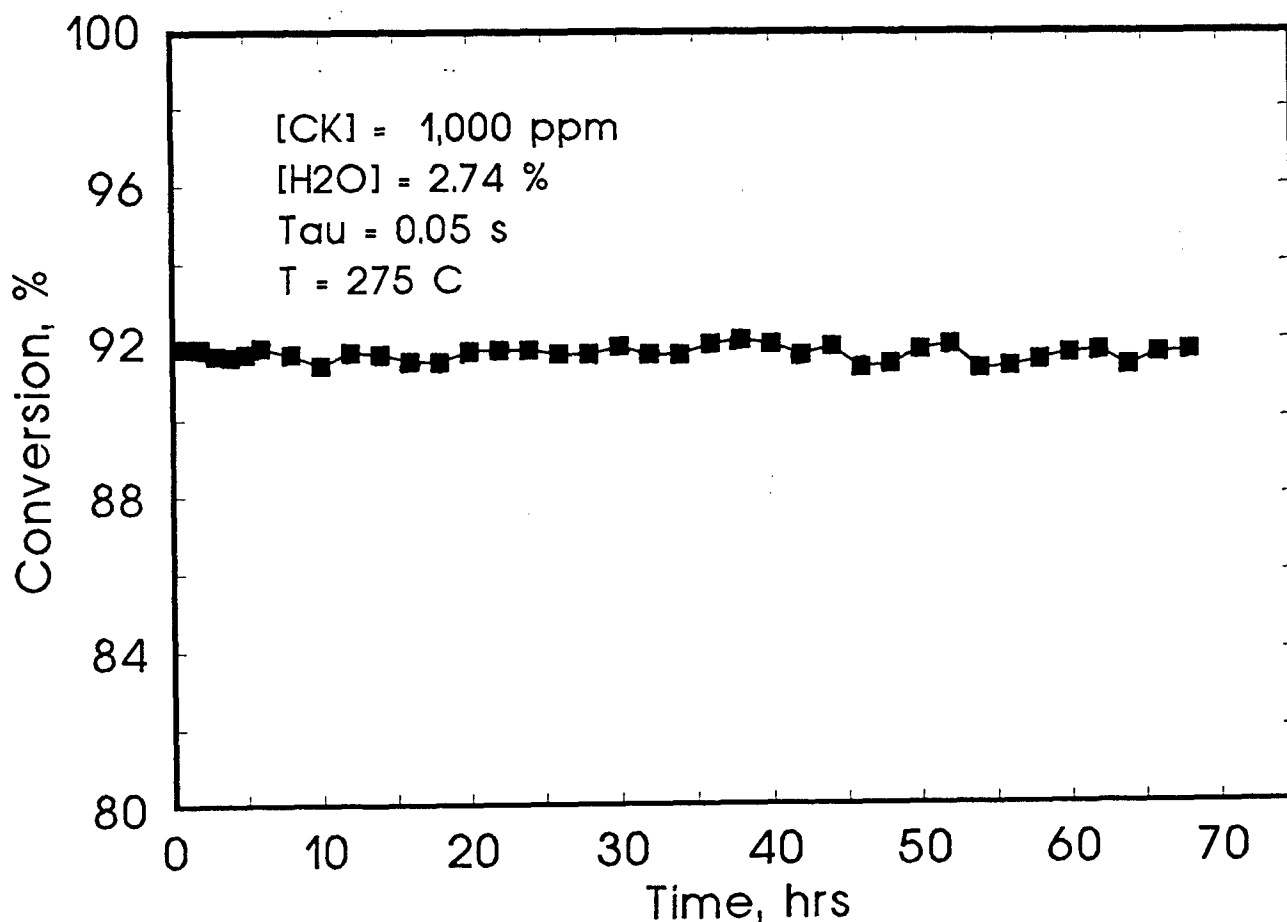


Figure 7: Conversion as a function of time-on-stream for the oxidation of 1,000 ppm cyanogen chloride in humid air at 275°C .

conversion of cyanogen chloride remain constant at about 92% throughout the duration of the run. During the run, 7.4 cm³ of monolith (about 0.85 g of washcoat) destroyed 99.6 g of cyanogen chloride. Results demonstrate that the catalyst is stable and will not be deactivated by exposure to cyanogen chloride.

Following completion of the run, the catalyst was exposed to dry air ($T_{\text{dew}} = < -35^{\circ}\text{C}$) at 400°C overnight in order to remove all traces of moisture from the system. The stability of the catalyst was then evaluated under dry conditions by exposing the catalyst to 1,000 ppm cyanogen chloride at 400°C at a residence time of 0.5 s. The results of this test are shown in Figure 8. The conversion of cyanogen chloride rapidly decreased over the first hour of the run. Following this time, the conversion continued to decrease, but at a slower rate. A comparison of results presented in Figures 7 and 8 highlights the effects of water on the performance of the catalyst. In dry air, increasing the reaction temperature by 125°C and decreasing the residence time by a factor of ten was required in order to achieve a meaningful conversion. Following this run, the catalyst was cooled to 275°C overnight in flowing, humid air. In the morning, the catalyst was exposed to 1,000 ppm cyanogen chloride at 275°C at a residence time of 0.05 s in humid air. The conversion of cyanogen chloride was approximate 90%, consistent with the conversion obtained prior to the dry air exposure. Interestingly, exposure of the catalyst to cyanogen chloride under dry conditions did not irreversibly deactivate the catalyst.

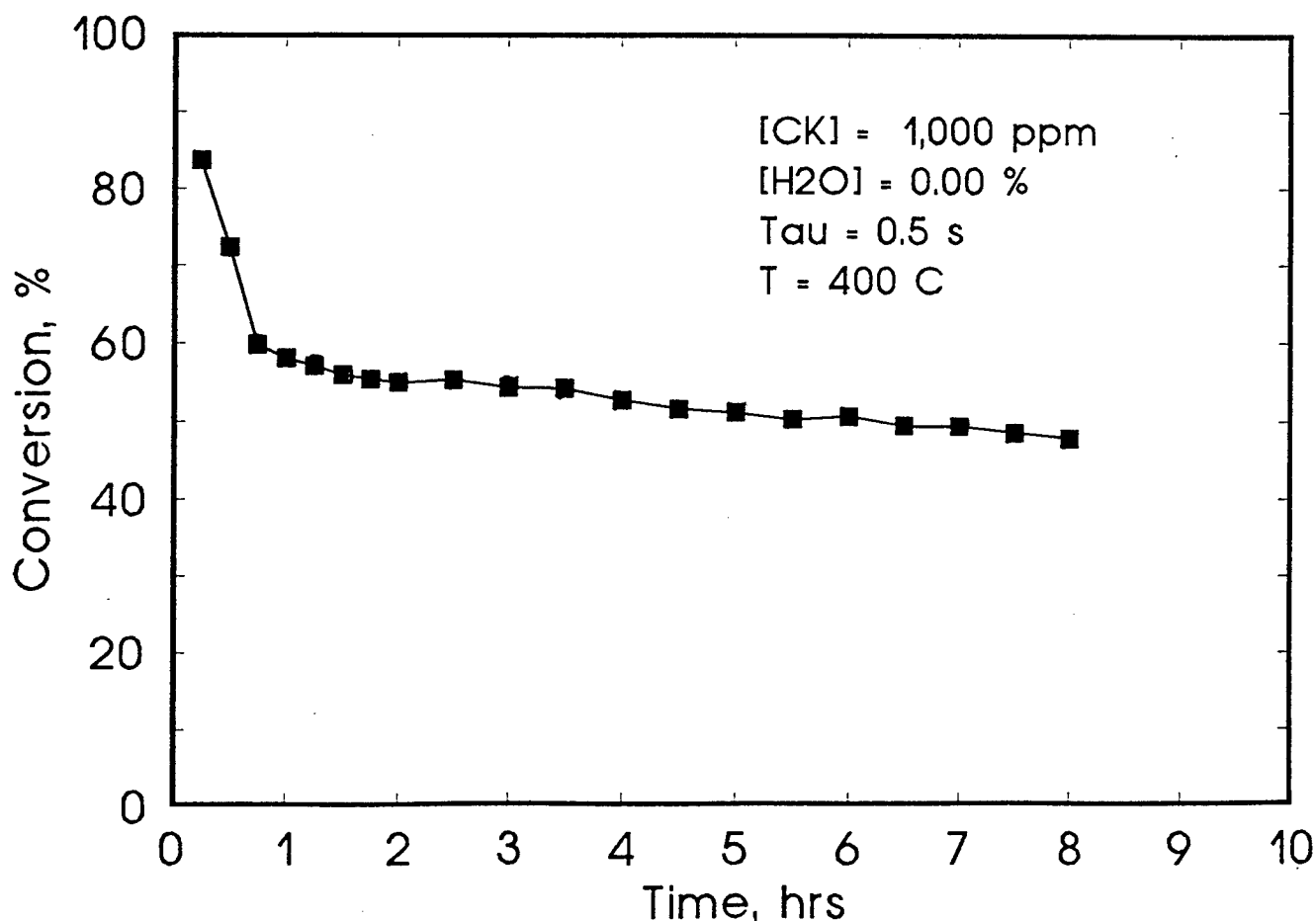


Figure 8: Conversion as a function of time-on-stream for the oxidation of 1,000 ppm cyanogen chloride in dry air at 400°C .

Reaction Rate Measurements: Axial temperature gradients were assessed during each run from temperature measurements obtained using thermocouples located within channels near the outer circumference of the monolith. Typically, the axial temperature deviation was less than 3-5°C, with the deviation increasing to 10°C for runs conducted with a 10,000 ppm feed concentration. Even the 10°C temperature deviation was not deemed to be unacceptable, and therefore data recorded under these conditions were used in the fit parameter analysis.

Reaction rate data were recorded at temperatures of 200, 250, 275 and 300°C for cyanogen chloride feed concentrations between 100 and 10,000 ppm (274 and 27,400 mg/m³) at 6±1 psig in humid ($T_{\text{dew}} = 23\pm1^\circ\text{C}$) air. Figures 9 through 12 report the conversion of cyanogen chloride as a function of residence time at reaction temperatures of 200, 250, 275 and 300°C, respectively. Results presented in these figures show that increasing the concentration of cyanogen chloride has a significant effect on conversion, especially at 200°C. For example, increasing the feed concentration of cyanogen chloride from 300 ppm to 1,000 ppm at 200°C at a residence time of 0.1 seconds results in the conversion decreasing from about 75% to about 50%. At higher reaction temperatures, the effects of increasing the cyanogen chloride feed concentration on conversion are present but less pronounced. Results indicate that the reaction is being inhibited by the adsorption of reactant and/or reaction product (HCl) on catalytic sites.

Several different forms of the reaction rate expression were evaluated for their ability to correlate the experimental data. The form of the reaction rate expression which best described the experimental data is reported as eq. 1. This rate expression takes into account the adsorption of cyanogen chloride and product hydrochloric acid on the reaction sites. Failure to account for the adsorption of hydrochloric acid resulted in a poor data correlation. The solid lines in the Figures 9 through 12 represent the data correlated using the reactor design equation (eqs. 2 and 3). Figure 13 shows a parity plot of the predicted and experimental conversion of cyanogen chloride. Results presented in Figures 9 through 13 demonstrates the ability of the design equation to accurately describe the experimental data.

The form of the reaction rate expression and the effects of water concentration (Figure 5) suggest that the reaction is occurring via a catalyzed hydrolysis reaction, with the reaction being inhibited by the presence of product hydrochloric acid. The reaction rate expression may be derived by assuming gas phase cyanogen chloride adsorbs onto surface hydroxyls and is subsequently decomposed, with the reaction being inhibited by the presence of HCl. It should be noted that the reaction rate expression did not take into account the effects of water. This is because data used to derive the rate expression were recorded under conditions in which the concentration of water did not affect the catalytic activity.

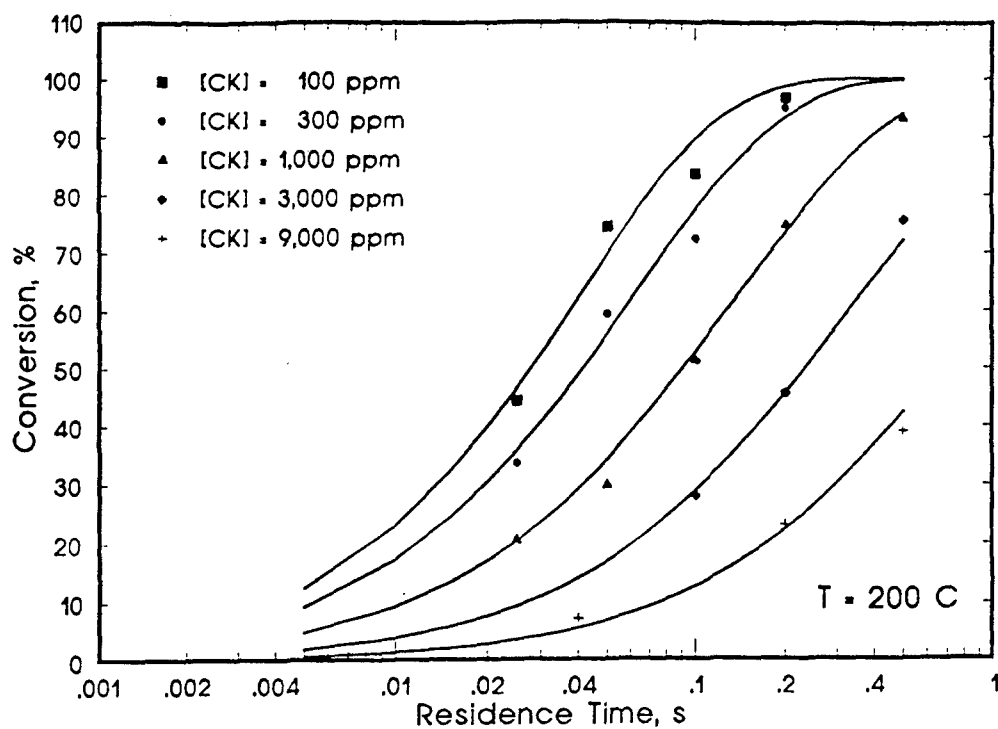


Figure 9: Conversion of cyanogen chloride as a function of residence time in humid air at 200°C. Solid lines represent data as correlated using the reactor design equation.

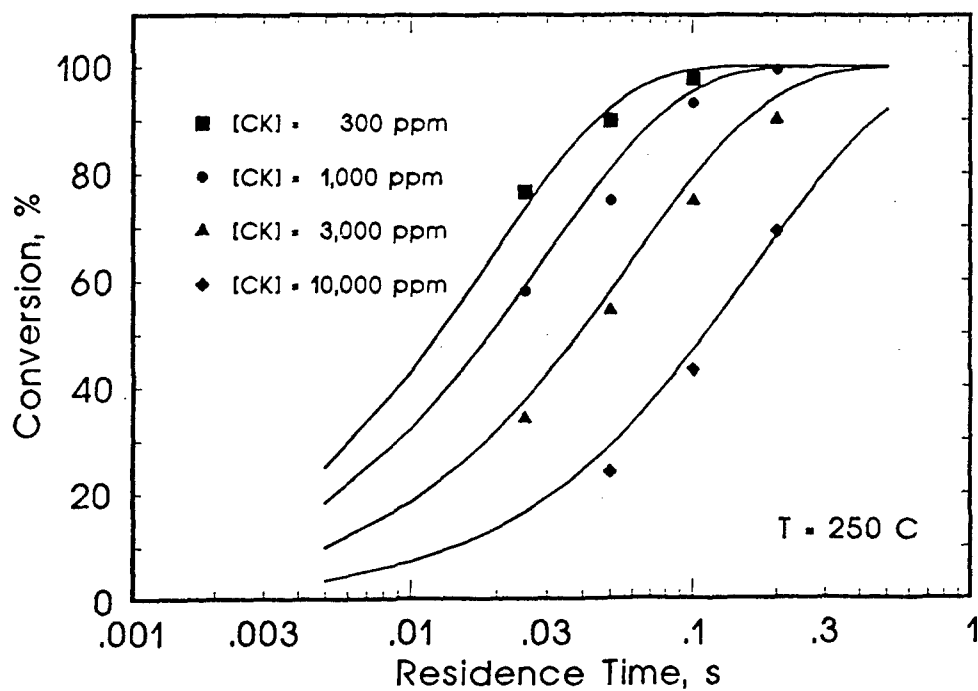


Figure 10: Conversion of cyanogen chloride as a function of residence time in humid air at 250°C. Solid lines represent data as correlated using the reactor design equation.

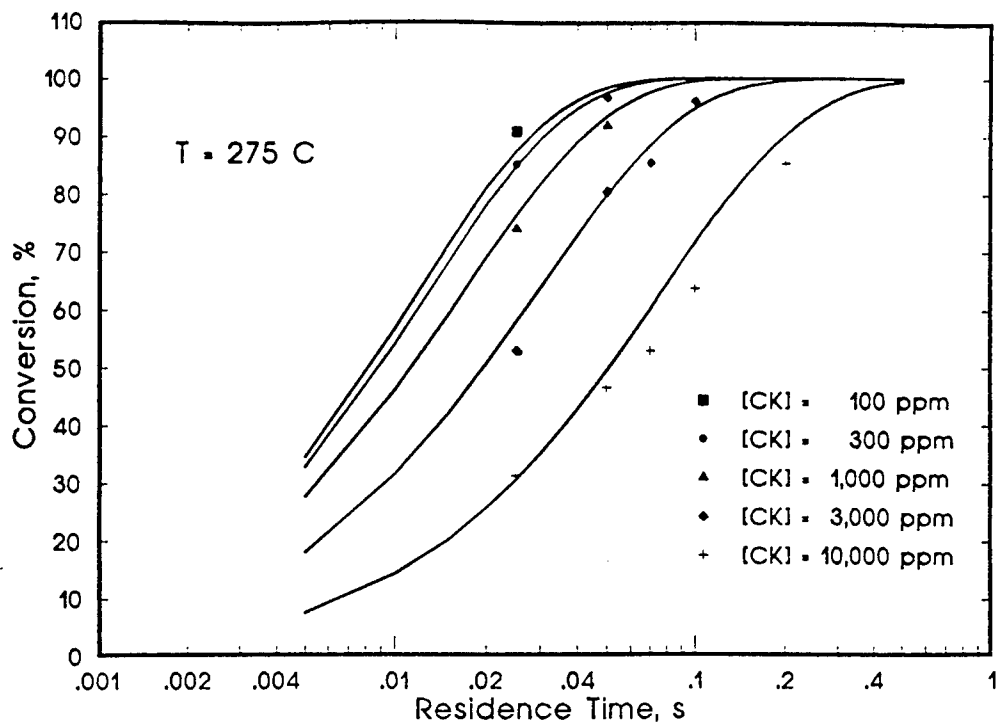


Figure 11: Conversion of cyanogen chloride as a function of residence time in humid air at 275°C. Solid lines represent data as correlated using the reactor design equation.

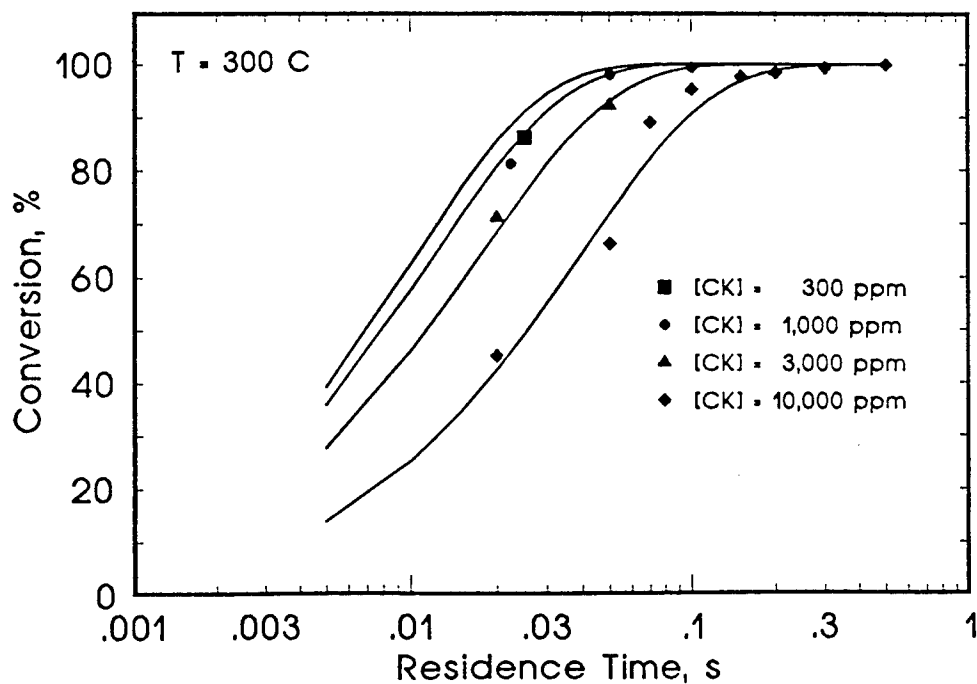


Figure 12: Conversion of cyanogen chloride as a function of residence time in humid air at 300°C. Solid lines represent data as correlated using the reactor design equation.

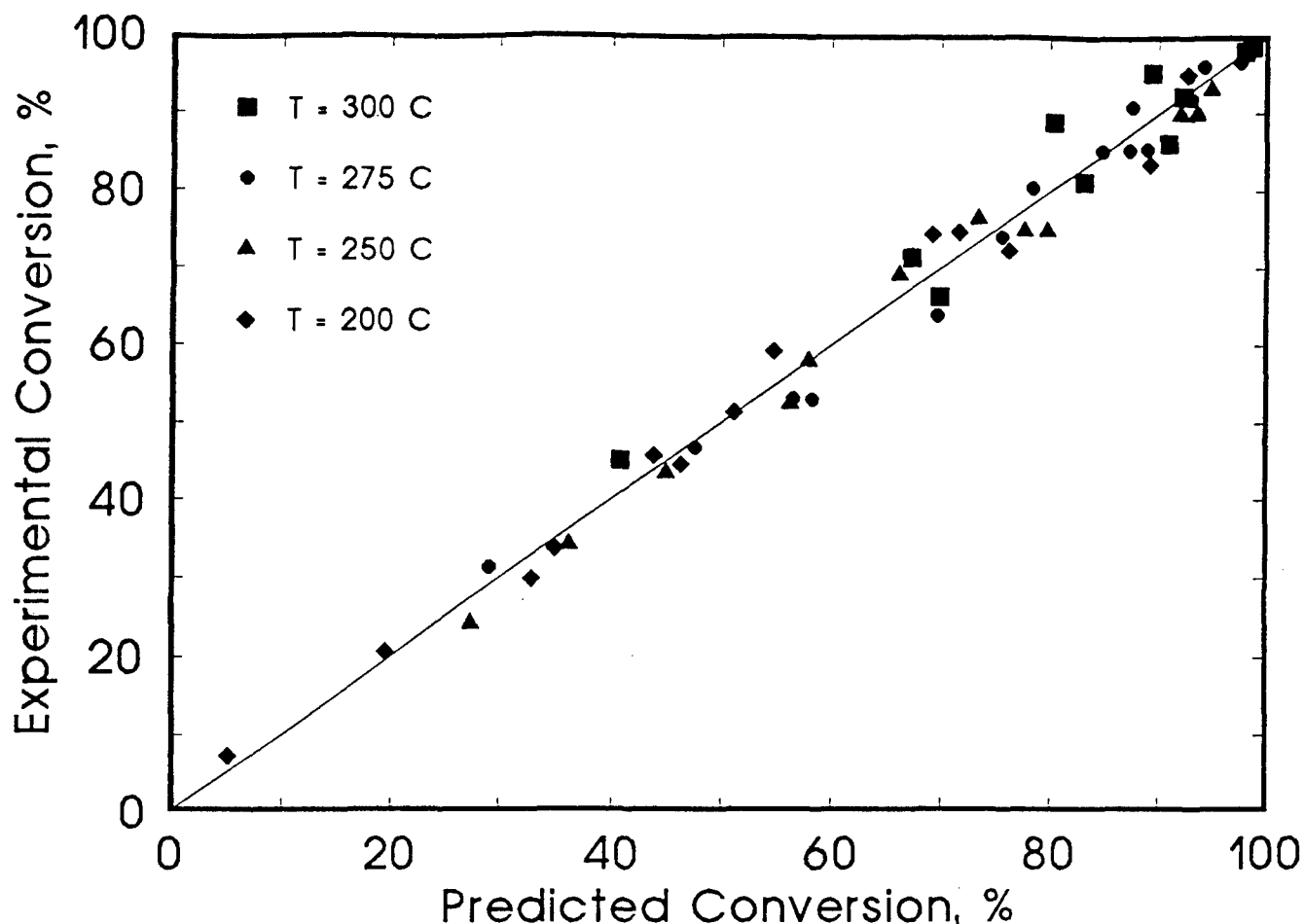


Figure 13: Parity plot of predicted versus experimental conversion of cyanogen chloride.

Figure 14 reports the conversion of cyanogen chloride as a function of residence time at 300°C. Data were recorded for feed concentrations of 3,000 and 10,000 ppm (9,133 and 27,400 mg/m³) and are reported for the purpose of evaluating the ability the model to predict conversions greater than 99%. The high conversion scenario was evaluated because military air purification systems require that the challenge be reduced by several orders of magnitude. The solid lines in Figure 14 represent the cyanogen chloride conversion predicted using the reactor design equation. Results presented in this figure demonstrate that the reactor design equation can be used to accurately predict cyanogen chloride reduction ratios up to four orders of magnitude (which was the detection limits of our instruments) under isothermal conditions.

5. CONCLUSIONS

Cyanogen chloride may be readily oxidized over the monolithic oxidation catalyst at temperatures greater than about 250°C. Reaction products consisted of CO₂, HCl, N₂, N₂O and NO_x, with the nitrogen product selectivity being a strong function of catalyst temperature. Catalytic deactivation was not observed under humid conditions, indicating that the catalyst is very stable. In the absence of water, catalyst deactivation was

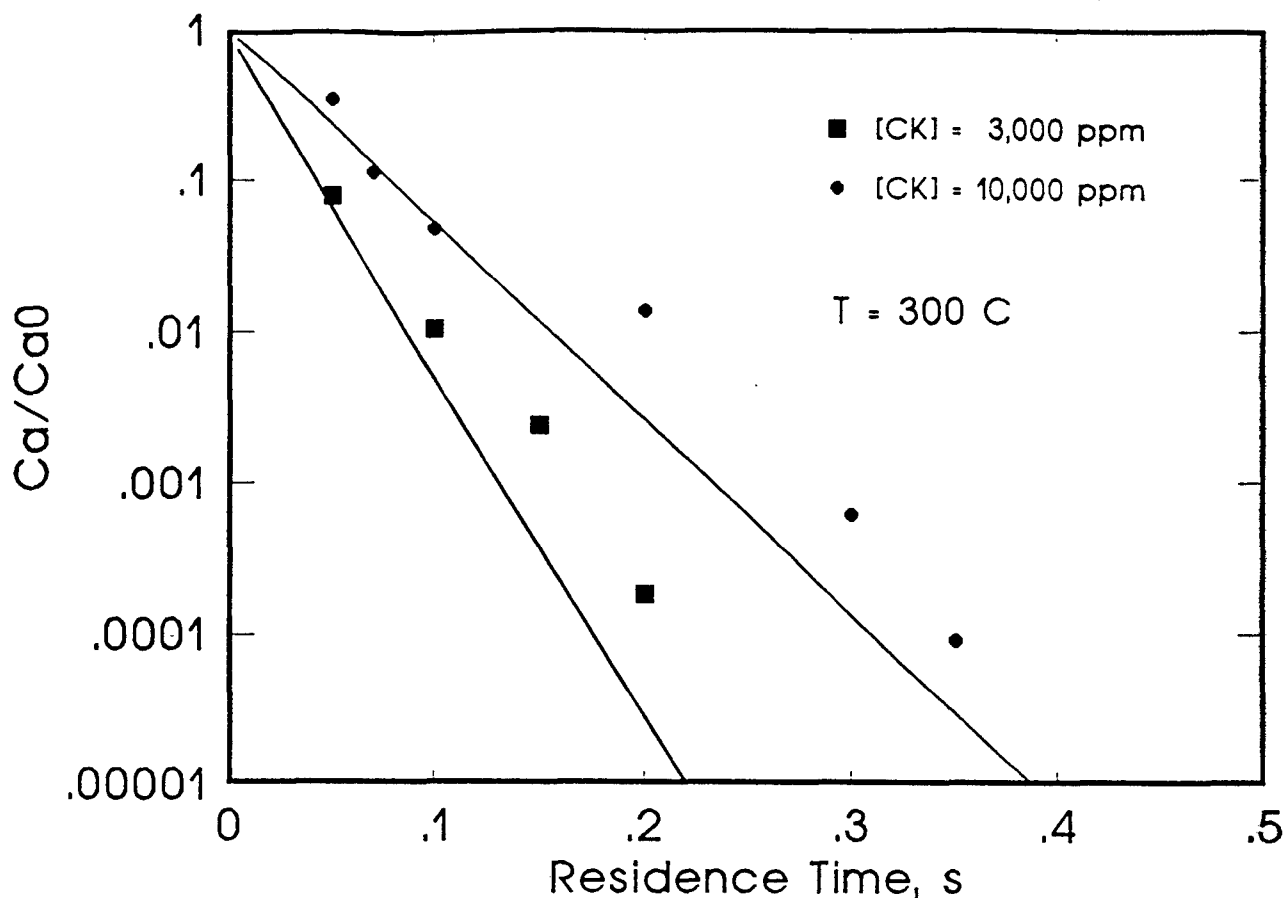


Figure 14: Reduction ratio, C_a / C_a^0 , of cyanogen chloride as a function of residence time at 300°C.

observed. For water vapor concentrations less than 0.10%, the presence of water in the feed had a significant effect on the activity of the catalyst. In the absence of water, the oxidation of cyanogen chloride was very slow, requiring reaction temperatures greater than 400°C in order to proceed. The addition of a small amount of water to the feed stream greatly enhanced the catalytic activity. For water vapor concentrations greater than 0.25%, the concentration of water in the feed stream did not, to within experimental error, affect the catalytic activity. Under isothermal conditions, the oxidation of cyanogen chloride could be modeled employing a reaction mechanism which assumes the reaction occurs via adsorption and decomposition of cyanogen chloride onto surface hydroxyl groups. The reactor design equation was able to accurately describe the conversion of cyanogen chloride over a wide range of process conditions.

Blank

LITERATURE CITED

- 1) Rossin, J.A., E. Petersen, D. E. Tevault, R. Lamontagne and L. Isaacson, "Effects of Environmental Weathering on the Properties of ASC Whetlerite," *Carbon*, **29**, 197 (1991).
- 2) Spivey, J.J.; *Complete Catalytic Oxidation of Volatile Organics*," *Ind. Eng. Chem. Res.* **26**, (1987) 2165.
- 3) Schmidt, T.; "*Industrial Applications of Catalysis for Offgas Treatment*," in *Catalysis and Automotive Pollution Control II*; Crucq, A. ed.; Elsevier: Amsterdam, 1991; p. 55.
- 4) Papenmeier, D. M. and Rossin, J.A., "*Catalytic Oxidation of Dichloromethane, Chloroform and Their Binary Mixtures Over a Platinum Alumina Catalyst*," *Ind. Eng. Chem. Res.* **33** (1994) 3094.
- 5) Chatterjee, S., Green, H. L. and Park, Y. J.; "*Comparison of Modified Transition Metal-Exchanged Zeolite Catalysts for Oxidation of Chlorinated Hydrocarbons*," *J. Catal.* **138**, (1992) 179.
- 6) Anderson, J. R. and McConkey, B. H.; "*Reactions of Methyl Chloride and of Methylene Chloride at Metal Surfaces*," *J. Catal.* **11**, (1968) 54.
- 7) Weldon, J. and Senkan, S. M.; "*Catalytic Oxidation of CH₃ by Cr₂O₃*," *Combust. Sci. Technol.* **47** (1986) 229.
- 8) Rossin, J. A. and Farris, M.M.; "*Catalytic Oxidation of Chloroform over a 2% Platinum Alumina Catalyst*," *Ind. Eng. Chem. Res.* **32**, (1993) 1024.
- 9) Klinghoffer, A.A and Rossin, J.A.; "*Catalytic Oxidation of Chloroacetonitrile over a 1% Platinum Alumina Catalyst*," *Ind. Eng. Chem. Res.* **31**, (1992) 481.
- 10) Lester, G. R. "*Catalytic Destruction of Organohalogen Compounds*," Int. Patent Appl. WO 90/13352, 1990.
- 11) Lester, G. L. and Homeyer, S. T.; "*Catalytic Destruction of Organic Volatile Nitrogen Compounds*," Am. Chem. Soc. National Meeting, Denver, Colorado, April, 1993.
- 12) Rossin, J.A.; "*Catalytic Oxidation of Hydrogen Cyanide Over a Monolithic Oxidation Catalyst*," U.S. Army ERDEC Technical Report ERDEC-CR-199, Aberdeen Proving Ground, MD (1995), Unclassified.

- 13) Campbell, J. M. and Rossin, J. A.; "Catalytic Oxidation of Volatile Nitrogen-Containing Compounds," 1995 AIChE National Meeting, Miami, Florida, November 1995.
- 14) Klinghoffer, A.A., Rossin, J.A. and Tevault, D.E.; "*Catalytic Oxidation of a CK Model Compound over a Monolithic Oxidation Catalyst*," U.S. Army ERDEC Technical Report ERDEC-CR-041, Aberdeen Proving Ground, MD (1993), Unclassified.
- 15) Irandoust, S. and B. Andersson, "Monolithic Catalysts for Nonautomobile Applications," *Catal. Rev. Sci. Eng.*, **30**, 341 (1988).
- 16) Froment, G. F. and K. B. Bischoff, Chemical Reactor Analysis and Design, Wiley: New York, 1979.
- 17) Stock, H.R. and Lowe, A., "Measurement and Differential Kinetic Analysis of Wall Temperatures in Monolith Converters-I," *Chem. Eng. Sci.*, **38** (1983) 1039.
- 18) Lowe, A. and Stock, H.R., "Measurement and Differential Kinetic Analysis of Wall Temperatures in Monolith Converters-II," *Chem. Eng. Sci.*, **39** (1984) 227.

Appendix

FORTRAN routine used to determine kinetic fit parameters

```

C-----
C This routine, MONO1.F, determines the kinetic fit parameters
C for the oxidation of compound in air over a monolith
C with a reaction rate expression:
C
C
C          ACa
C      Rate = -----
C          (1 + BCp + DCa)
C
C   Where:
C     A, B and D are fit parameters
C     Ca is the reactant concentration
C     Cp is the concentration of reaction product
C
C The reaction is modeled according to:
C
C   v dCa/dz = kA(Ca,g - Ca,s)
C   Rate = kA(Ca,s - Ca,g)
C
C   Where v is the velocity, z is the reactor length, k is
C   the mass transfer coefficient, and A is the surface area
C   of the monolith. The subscripts s and g refer to the
C   gas and solid phase.
C-----
      IMPLICIT REAL*8 (A-H,O-Z)
      DIMENSION Y0(5), CONV(100), A1(6,7), P5(6)
      DIMENSION CONX(30), X(100)
      COMMON /SBCOM1/ XKM1, SA, SS, CA0, RHOB
      COMMON /SBCOM3/ X1, X2, X3
      COMMON /SBCOM2/ WASHT, CELLR, TOUT, VEL
      common /sbcom3/ j, j5
      DATA ONE /1.0D00/, TWO /2.0D00/, FOUR /4.0D00/, ZERO /0.0D00/
      DATA RG /82.085D00/, KORD /2/, KORD1 /3/
C-----
C   N is the number of equations to be solved by EPISODE
C-----
      N = 1

      OPEN(9,FILE='stat.out')
      OPEN(7,FILE='test.out')
      OPEN(5, FILE='mono1.dat')
      REWIND(5)
C-----
C   NDAT is the number of data points.
C   A0, B0 and D0 are initial guesses for the pre-exponential factors
C   corresponding to the fit parameters X1, X2 and X3. EA, EB and
C   ED are initial guesses for the corresponding activation energies.
C-----
      READ(5,28) NDAT, A0, B0, D0, EA, EB, ED
28  FORMAT(17,/,D18.8,/,D18.8,/,D18.8,/,D18.8,/,D18.8,/,D18.8)
      READ(5,26) RHOB, SAVEH, TOUT, EPS

```



```

      READ(5,27) TREF,PRESS,CELLR,WASHT,SUBT,XKM
      READ(5,27) DELA,DELB,DELD,DEL1,DEL2,DEL4
26  FORMAT(3(D18.8,/),D18.8)
27  FORMAT(5(D18.8,/),D18.8)
      CLOSE(5)
      DELA = A0/DELA
      DELB = B0/DELB
      DELD = D0/DELD
      DEL1 = EA/DEL1
      DEL2 = EB/DEL2
      DEL4 = ED/DEL4
C-----
C   SS   surface area, cm**2 catalyst/cm**3 reactor void
C   SA   surface area, cm**2 catalyst/cm**3 catalyst
C-----
      CELLR = CELLR - SUBT
      CELLT = CELLR - TWO*WASHT
      SS = FOUR/CELLT
      SA = FOUR*CELLT/((CELLR*CELLR - CELLT*CELLT)
      VOID = (CELLT*CELLT)/((CELLR+SUBT)*(CELLR+SUBT))
C-----
c The DO 600 loop is used to re-evaluate the function with a
c new set of fit parameters
C-----
      DO 600 L = 1,50
      F1 = ZERO
      F2 = ZERO
      F3 = ZERO
      F4 = ZERO
      F5 = ZERO
      F6 = ZERO
      F1A = ZERO
      F1B = ZERO
      F1D = ZERO
      F11 = ZERO
      F12 = ZERO
      F14 = ZERO
      F2A = ZERO
      F2B = ZERO
      F2D = ZERO
      F21 = ZERO
      F22 = ZERO
      F24 = ZERO
      F3A = ZERO
      F3B = ZERO
      F3D = ZERO
      F31 = ZERO
      F32 = ZERO
      F34 = ZERO
      F4A = ZERO
      F4B = ZERO
      F4D = ZERO
      F41 = ZERO
      F42 = ZERO

```

```

F44 = ZERO
F5A = ZERO
F5B = ZERO
F5D = ZERO
F51 = ZERO
F52 = ZERO
F54 = ZERO
F6A = ZERO
F6B = ZERO
F6D = ZERO
F61 = ZERO
F62 = ZERO
F64 = ZERO
OPEN(2,FILE='ck.dat')
rewind(2)
c-----
c The DO 500 loop calculates conversions at a fixed set of process
c conditions, varying the fit parameters accordingly.
c-----
      DO 500 J = 1,NDAT
        READ(2,12) TAU, TEMP, CONC, CONV(J)
        XKM1 = XKM*(TEMP/573.15D00)**1.5D00
        VEL = TOUT*TEMP/(VOID*273.15D00*PRESS*TAU)
        CA0 = CONC
        TX = (ONE/TEMP - ONE/TREF)
12  FORMAT(4D12.6)
        DO 400 J5 = 1,28
          IF(J5.EQ.1) THEN
            X1 = A0*DEXP(-EA*TX)
            X2 = B0*DEXP(EB*TX)
            X3 = D0*DEXP(ED*TX)
          ELSE
            ENDIF
          IF(J5.EQ.2) THEN
            X1 = (A0 + DELA)*DEXP(-EA*TX)
            X2 = B0*DEXP(EB*TX)
            X3 = D0*DEXP(ED*TX)
          ELSE
            ENDIF
          IF(J5.EQ.3) THEN
            X1 = (A0 - DELA)*DEXP(-EA*TX)
            X2 = B0*DEXP(EB*TX)
            X3 = D0*DEXP(ED*TX)
          ELSE
            ENDIF
          IF(J5.EQ.4) THEN
            X1 = A0*DEXP(-EA*TX)
            X2 = (B0 + DELB)*DEXP(EB*TX)
            X3 = D0*DEXP(ED*TX)
          ELSE
            ENDIF
          IF(J5.EQ.5) THEN
            X1 = A0*DEXP(-EA*TX)
            X2 = (B0 - DELB)*DEXP(EB*TX)

```

```

      X3 = D0*DEXP(ED*TX)
ELSE
ENDIF
IF(J5.EQ.6) THEN
  X1 = A0*DEXP(-EA*TX)
  X2 = B0*DEXP(EB*TX)
  X3 = (D0 + DELD)*DEXP(ED*TX)
ELSE
ENDIF
IF(J5.EQ.7) THEN
  X1 = A0*DEXP(-EA*TX)
  X2 = B0*DEXP(EB*TX)
  X3 = (D0 - DELD)*DEXP(ED*TX)
ELSE
ENDIF
IF(J5.EQ.8) THEN
  X1 = A0*DEXP(-(EA+DEL1)*TX)
  X2 = B0*DEXP(EB*TX)
  X3 = D0*DEXP(ED*TX)
ELSE
ENDIF
IF(J5.EQ.9) THEN
  X1 = A0*DEXP(-(EA-DEL1)*TX)
  X2 = B0*DEXP(EB*TX)
  X3 = D0*DEXP(ED*TX)
ELSE
ENDIF
IF(J5.EQ.10) THEN
  X1 = A0*DEXP(-EA*TX)
  X2 = B0*DEXP((EB+DEL2)*TX)
  X3 = D0*DEXP(ED*TX)
ELSE
ENDIF
IF(J5.EQ.11) THEN
  X1 = A0*DEXP(-EA*TX)
  X2 = B0*DEXP((EB-DEL2)*TX)
  X3 = D0*DEXP(ED*TX)
ELSE
ENDIF
IF(J5.EQ.12) THEN
  X1 = A0*DEXP(-EA*TX)
  X2 = B0*DEXP(EB*TX)
  X3 = D0*DEXP((ED+DEL4)*TX)
ELSE
ENDIF
IF(J5.EQ.13) THEN
  X1 = A0*DEXP(-EA*TX)
  X2 = B0*DEXP(EB*TX)
  X3 = D0*DEXP((ED-DEL4)*TX)
ELSE
ENDIF
IF(J5.EQ.14) THEN
  X1 = (A0 + DELA)*DEXP(-EA*TX)
  X2 = (B0 + DELB)*DEXP(EB*TX)

```

```

    X3 = D0*DEXP(ED*TX)
ELSE
ENDIF
IF(J5.EQ.15) THEN
    X1 = (A0 + DELA)*DEXP(-EA*TX)
    X2 = B0*DEXP(EB*TX)
    X3 = (D0 + DELD)*DEXP(ED*TX)
ELSE
ENDIF
IF(J5.EQ.16) THEN
    X1 = (A0 + DELA)*DEXP(-(EA+DEL1)*TX)
    X2 = B0*DEXP(EB*TX)
    X3 = D0*DEXP(ED*TX)
ELSE
ENDIF
IF(J5.EQ.17) THEN
    X1 = (A0 + DELA)*DEXP(-EA*TX)
    X2 = B0*DEXP((EB+DEL2)*TX)
    X3 = D0*DEXP(ED*TX)
ELSE
ENDIF
IF(J5.EQ.18) THEN
    X1 = (A0 + DELA)*DEXP(-EA*TX)
    X2 = B0*DEXP(EB*TX)
    X3 = D0*DEXP((ED+DEL4)*TX)
ELSE
ENDIF
IF(J5.EQ.19) THEN
    X1 = A0*DEXP(-EA*TX)
    X2 = (B0 + DELB)*DEXP(EB*TX)
    X3 = (D0 + DELD)*DEXP(ED*TX)
ELSE
ENDIF
IF(J5.EQ.20) THEN
    X1 = A0*DEXP(-(EA+DEL1)*TX)
    X2 = (B0 + DELB)*DEXP(EB*TX)
    X3 = D0*DEXP(ED*TX)
ELSE
ENDIF
IF(J5.EQ.21) THEN
    X1 = A0*DEXP(-EA*TX)
    X2 = (B0 + DELB)*DEXP((EB+DEL2)*TX)
    X3 = D0*DEXP(ED*TX)
ELSE
ENDIF
IF(J5.EQ.22) THEN
    X1 = A0*DEXP(-EA*TX)
    X2 = (B0 + DELB)*DEXP(EB*TX)
    X3 = D0*DEXP((ED+DEL4)*TX)
ELSE
ENDIF
IF(J5.EQ.23) THEN
    X1 = A0*DEXP(-(EA+DEL1)*TX)
    X2 = B0*DEXP(EB*TX)

```

```

      X3 = (D0 + DELD)*DEXP(ED*TX)
    ELSE
    ENDIF
  IF(J5.EQ.24) THEN
    X1 = A0*DEXP(-EA*TX)
    X2 = B0*DEXP((EB+DEL2)*TX)
    X3 = (D0 + DELD)*DEXP(ED*TX)
  ELSE
  ENDIF
  IF(J5.EQ.25) THEN
    X1 = A0*DEXP(-EA*TX)
    X2 = B0*DEXP(EB*TX)
    X3 = (D0 + DELD)*DEXP((ED+DEL4)*TX)
  ELSE
  ENDIF
  IF(J5.EQ.26) THEN
    X1 = A0*DEXP(-(EA+DEL1)*TX)
    X2 = B0*DEXP((EB+DEL2)*TX)
    X3 = D0*DEXP(ED*TX)
  ELSE
  ENDIF
  IF(J5.EQ.27) THEN
    X1 = A0*DEXP(-(EA+DEL1)*TX)
    X2 = B0*DEXP(EB*TX)
    X3 = D0*DEXP((ED+DEL4)*TX)
  ELSE
  ENDIF
  IF(J5.EQ.28) THEN
    X1 = A0*DEXP(-EA*TX)
    X2 = B0*DEXP((EB+DEL2)*TX)
    X3 = D0*DEXP((ED+DEL4)*TX)
  ELSE
  ENDIF

```

c-----

c setting initial conditions at reactor entrance

c-----

Y0(1) = 1.0D00

c-----

c EPISODE error control

c IERROR = 1 Absolute error control, Ymax(i) = 1

c IERROR = 2 Error relative to Y(i) is controlled.

c If Y(i) = 0, a divide error occurs

c IERROR = 3 Error relative to the largest value of

c Y(i) is controlled.

c-----

IERROR = 1

T0 = 0.0D00

MF = 22

INDEX = 1

H0 = SAVEH

CALL DRIVE(N, T0, H0, Y0, TOUT, EPS, IERROR, MF, INDEX)

CONX(J5) = (ONE - Y0(1))*100.0D00

```

      IF(J5.EQ.1) THEN
        X(J) = CONX(1)
        WRITE(*,129) X(J), CONV(J)
        WRITE(9,129) X(J), CONV(J)
        SUM = SUM + (X(J)-CONV(J))*(X(J)-CONV(J))
      ELSE
        ENDIF
400  CONTINUE
      PA = (CONX(2) - CONX(1))/DELA
      PB = (CONX(4) - CONX(1))/DELB
      PD = (CONX(6) - CONX(1))/DELD
      P1 = (CONX(8) - CONX(1))/DEL1
      P2 = (CONX(10) - CONX(1))/DEL2
      P4 = (CONX(12) - CONX(1))/DEL4
      PAA = (CONX(2) - TWO*CONX(1) + CONX(3))/(DELA*DELA)
      PBB = (CONX(4) - TWO*CONX(1) + CONX(5))/(DELB*DELB)
      PDD = (CONX(6) - TWO*CONX(1) + CONX(7))/(DELD*DELD)
      P11 = (CONX(8) - TWO*CONX(1) + CONX(9))/(DEL1*DEL1)
      P22 = (CONX(10) - TWO*CONX(1) + CONX(11))/(DEL2*DEL2)
      P44 = (CONX(12) - TWO*CONX(1) + CONX(13))/(DEL4*DEL4)
      PAB = (CONX(1) - CONX(2) - CONX(4) + CONX(14))/(DELA*DELB)
      PAD = (CONX(1) - CONX(2) - CONX(6) + CONX(15))/(DELA*DELD)
      PA1 = (CONX(1) - CONX(2) - CONX(8) + CONX(16))/(DELA*DEL1)
      PA2 = (CONX(1) - CONX(2) - CONX(10) + CONX(17))/(DELA*DEL2)
      PA4 = (CONX(1) - CONX(2) - CONX(12) + CONX(18))/(DELA*DEL4)
      PBD = (CONX(1) - CONX(4) - CONX(6) + CONX(19))/(DELB*DELD)
      PB1 = (CONX(1) - CONX(4) - CONX(8) + CONX(20))/(DELB*DEL1)
      PB2 = (CONX(1) - CONX(4) - CONX(10) + CONX(21))/(DELB*DEL2)
      PB4 = (CONX(1) - CONX(4) - CONX(12) + CONX(22))/(DELB*DEL4)
      PD1 = (CONX(1) - CONX(6) - CONX(8) + CONX(23))/(DELD*DEL1)
      PD2 = (CONX(1) - CONX(6) - CONX(10) + CONX(24))/(DELD*DEL2)
      PD4 = (CONX(1) - CONX(6) - CONX(12) + CONX(25))/(DELD*DEL4)
      P12 = (CONX(1) - CONX(8) - CONX(10) + CONX(26))/(DEL1*DEL2)
      P14 = (CONX(1) - CONX(8) - CONX(12) + CONX(27))/(DEL1*DEL4)
      P24 = (CONX(1) - CONX(10) - CONX(12) + CONX(28))/(DEL2*DEL4)

      F1 = F1 + TWO*CONV(J)*PA - TWO*CONX(1)*PA
      F2 = F2 + TWO*CONV(J)*PB - TWO*CONX(1)*PB
      F3 = F3 + TWO*CONV(J)*PD - TWO*CONX(1)*PD
      F4 = F4 + TWO*CONV(J)*P1 - TWO*CONX(1)*P1
      F5 = F5 + TWO*CONV(J)*P2 - TWO*CONX(1)*P2
      F6 = F6 + TWO*CONV(J)*P4 - TWO*CONX(1)*P4

      F1A = F1A + TWO*(CONV(J)*PAA - CONX(1)*PAA - PA*PA)
      F1B = F1B + TWO*(CONV(J)*PAB - CONX(1)*PAB - PA*PB)
      F1D = F1D + TWO*(CONV(J)*PAD - CONX(1)*PAD - PA*PD)
      F11 = F11 + TWO*(CONV(J)*PA1 - CONX(1)*PA1 - PA*P1)
      F12 = F12 + TWO*(CONV(J)*PA2 - CONX(1)*PA2 - PA*P2)
      F14 = F14 + TWO*(CONV(J)*PA4 - CONX(1)*PA4 - PA*P4)

      F2A = F2A + TWO*(CONV(J)*PAB - CONX(1)*PAB - PB*PA)
      F2B = F2B + TWO*(CONV(J)*PBB - CONX(1)*PBB - PB*PB)
      F2D = F2D + TWO*(CONV(J)*PBD - CONX(1)*PBD - PB*PD)
      F21 = F21 + TWO*(CONV(J)*PB1 - CONX(1)*PB1 - PB*P1)

```

F22 = F22 + TWO*(CONV(J)*PB2 - CONX(1)*PB2 -PB*P2)
F24 = F24 + TWO*(CONV(J)*PB4 - CONX(1)*PB4 -PB*P4)

F3A = F3A + TWO*(CONV(J)*PAD - CONX(1)*PAD -PD*PA)
F3B = F3B + TWO*(CONV(J)*PBD - CONX(1)*PBD -PD*PB)
F3D = F3D + TWO*(CONV(J)*PDD - CONX(1)*PDD -PD*PD)
F31 = F31 + TWO*(CONV(J)*PD1 - CONX(1)*PD1 -PD*P1)
F32 = F32 + TWO*(CONV(J)*PD2 - CONX(1)*PD2 -PD*P2)
F34 = F34 + TWO*(CONV(J)*PD4 - CONX(1)*PD4 -PD*P4)

F4A = F4A + TWO*(CONV(J)*PA1 - CONX(1)*PA1 -P1*PA)
F4B = F4B + TWO*(CONV(J)*PB1 - CONX(1)*PB1 -P1*PB)
F4D = F4D + TWO*(CONV(J)*PD1 - CONX(1)*PD1 -P1*PD)
F41 = F41 + TWO*(CONV(J)*P11 - CONX(1)*P11 -P1*P1)
F42 = F42 + TWO*(CONV(J)*P12 - CONX(1)*P12 -P1*P2)
F44 = F44 + TWO*(CONV(J)*P14 - CONX(1)*P14 -P1*P4)

F5A = F5A + TWO*(CONV(J)*PA2 - CONX(1)*PA2 -P2*PA)
F5B = F5B + TWO*(CONV(J)*PB2 - CONX(1)*PB2 -P2*PB)
F5D = F5D + TWO*(CONV(J)*PD2 - CONX(1)*PD2 -P2*PD)
F51 = F51 + TWO*(CONV(J)*P12 - CONX(1)*P12 -P2*P1)
F52 = F52 + TWO*(CONV(J)*P22 - CONX(1)*P22 -P2*P2)
F54 = F54 + TWO*(CONV(J)*P24 - CONX(1)*P24 -P2*P4)

F6A = F6A + TWO*(CONV(J)*PA4 - CONX(1)*PA4 -P4*PA)
F6B = F6B + TWO*(CONV(J)*PB4 - CONX(1)*PB4 -P4*PB)
F6D = F6D + TWO*(CONV(J)*PD4 - CONX(1)*PD4 -P4*PD)
F61 = F61 + TWO*(CONV(J)*P14 - CONX(1)*P14 -P4*P1)
F62 = F62 + TWO*(CONV(J)*P24 - CONX(1)*P24 -P4*P2)
F64 = F64 + TWO*(CONV(J)*P44 - CONX(1)*P44 -P4*P4)

500 CONTINUE

100 CONTINUE

A1(1,7) = -F1
A1(2,7) = -F2
A1(3,7) = -F3
A1(4,7) = -F4
A1(5,7) = -F5
A1(6,7) = -F6
A1(1,1) = F1A
A1(1,2) = F1B
A1(1,3) = F1D
A1(1,4) = F11
A1(1,5) = F12
A1(1,6) = F14
A1(2,1) = F2A
A1(2,2) = F2B
A1(2,3) = F2D
A1(2,4) = F21
A1(2,5) = F22
A1(2,6) = F24
A1(3,1) = F3A
A1(3,2) = F3B
A1(3,3) = F3D

```

A1(3,4) = F31
A1(3,5) = F32
A1(3,6) = F34
A1(4,1) = F4A
A1(4,2) = F4B
A1(4,3) = F4D
A1(4,4) = F41
A1(4,5) = F42
A1(4,6) = F44
A1(5,1) = F5A
A1(5,2) = F5B
A1(5,3) = F5D
A1(5,4) = F51
A1(5,5) = F52
A1(5,6) = F54
A1(6,1) = F6A
A1(6,2) = F6B
A1(6,3) = F6D
A1(6,4) = F61
A1(6,5) = F62
A1(6,6) = F64
206 format(7d10.4)
CALL GAUSS(KORD, KORD1, A1, P5)

AOLD = A0
BOLD = B0
DOLD = D0
OLD1 = EA
OLD2 = EB
OLD4 = ED
A0 = A0 + P5(1)
B0 = B0 + P5(2)
D0 = D0 + P5(3)
EA = EA + P5(4)
EB = EB + P5(5)
ED = ED + P5(6)
EA0 = ((AOLD - A0)/A0)*((AOLD - A0)/A0)
EB0 = ((BOLD - B0)/B0)*((BOLD - B0)/B0)
ED0 = ((DOLD - D0)/D0)*((DOLD - D0)/D0)
EEA = ((OLD1 - EA)/EA)*((OLD1 - EA)/EA)
EEB = ((OLD2 - EB)/EB)*((OLD2 - EB)/EB)
EED = ((OLD4 - ED)/ED)*((OLD4 - ED)/ED)
IF(A0.gt.2.0D00*AOLD) A0 = 2.0D00*AOLD
IF(A0.lt.0.5D00*AOLD) A0 = 0.5D00*AOLD
IF(B0.gt.2.0D00*BOLD) B0 = 2.0D00*BOLD
IF(B0.lt.0.5D00*BOLD) B0 = 0.5D00*BOLD
IF(D0.gt.2.0D00*DOLD) D0 = 2.0D00*DOLD
IF(D0.lt.0.5D00*DOLD) D0 = 0.5D00*DOLD
IF(EA.gt.1.2D00*OLD1) EA = 1.2D00*OLD1
IF(EA.lt.0.8D00*OLD1) EA = 0.8D00*OLD1
IF(EB.gt.1.2D00*OLD2) EB = 1.2D00*OLD2
IF(EB.lt.0.8D00*OLD2) EB = 0.8D00*OLD2
IF(ED.gt.1.2D00*OLD4) ED = 1.2D00*OLD4
IF(ED.lt.0.8D00*OLD4) ED = 0.8D00*OLD4

```



```

SUME = dsqrt(EA0+EB0+ED0+EEA+EEB+EED)/5.0D00
ERROR = DSQRT(SUM)/DBLE(NDAT-1)
WRITE(*, 551) ERROR
WRITE(9, 551) ERROR
WRITE(*, 547) A0, B0, D0, EA, EB, ED, SUME
WRITE(9, 547) A0, B0, D0, EA, EB, ED, SUME
SUM = 0.0D00
IF(SUME.LT.1.0D-04) GOTO 699
600 CONTINUE
699 CONTINUE
800 CONTINUE
547 FORMAT(/,2X,'A0 = ',D12.6,2X,'B0 = ',D12.6,2X,'D0 = ',D12.6,/,
1      2X,'EA = ',D12.6,2X,'EB = ',D12.6,2X,'ED = ',D12.6,/,
1      2X,'ERROR = ',d12.6,/)
551 FORMAT(/2X,'XNORM = ',F8.5)
119 FORMAT(2X,'Conversion: ',f10.4)
129 FORMAT(2X,'Pred. Conv: ',f10.4,2X,'Exp. Conv: ',f10.4)
999 CONTINUE
    close(9)
    STOP
    END

```

```

SUBROUTINE GAUSS(KORD,KORD1,A,P5)
IMPLICIT REAL*8 (A-H,O-Z)
DIMENSION A(6,7), P5(7)
KORD = 6
KORD1 = KORD + 1
KORD2 = KORD - 1
DO 100 N1 = 1,KORD
    N3 = N1 + 1
    DO 101 N2 = N3,KORD
        IF(DABS(A(N2,N1)).GT.DABS(A(N1,N1))) GOTO 105
        GOTO 101
105    DO 106 I = 1,KORD1
        SAVE1 = A(N2,I)
        SAVE2 = A(N1,I)
        A(N1,I) = SAVE1
106    A(N2,I) = SAVE2
101    CONTINUE
        DO 115 N = N1,KORD
            ASAVE = A(N,N1)
            IF(DABS(ASAVE).LE.1.0D-50) GOTO 115
            DO 116 M = N1,KORD1
                A(N,M) = A(N,M)/ASAVE
116        CONTINUE
115        CONTINUE
            IF(N1.EQ.KORD) GOTO 100
            NEQ = N1 + 1
            DO 120 N = NEQ,KORD
                IF(DABS(A(N,N1)).LE.1.0D-50) GOTO 120
                DO 121 N2 = N1,KORD1
                    IF(DABS(A(N1,N)).LE.1.0D-50) GOTO 121
                    A(N,N2) = A(N1,N2) - A(N,N2)
121                CONTINUE

```

```

120    CONTINUE
100    CONTINUE
      P5(KORD) = A(KORD,KORD1)
      DO 200 N = 1,KORD2
        RHS = 0.0D00
        DO 210 I = 1,N
          210    RHS = P5(KORD1-I)*A(KORD-N,KORD1-I) + RHS
        200    P5(KORD-N) = A(KORD-N,KORD1) - RHS
      RETURN
      END

      SUBROUTINE DIFFUN (N, T, Y, YDOT)
      IMPLICIT REAL*8 (A-H, O-Z)
      DIMENSION Y(N), YDOT(N)
      COMMON /SBCOM1/ XKM1, SA, SS, CA0, RHOB
      COMMON /SBCOM3/ X1, X2, X3
      COMMON /SBCOM2/ WASHT, CELLR, TOUT, VEL
      common /sbcom3/ j, j5
      DATA PT5 /0.5D00/, ONE /1.0D00/, TWO /2.0D00/, FOUR /4.0D00/

```

```

c-----
c The surface concentration of HCN, XAS, is determined using
c Newton's method of iteration, where
c
c   0 = XKM1*SA*(Y(1) - XAS) - Rate == f(XAS)
c
c   XAS = Y(1)
15  FORMAT(2X,'XAS CONVERGENCE FAILURE, XAS = ',D12.6/,
1    2X,'ERROR = ',D12.6)

```

```

C-----
C   SS   surface area, cm**2 catalyst/cm**3 reactor void
C   SA   surface area, cm**2 catalyst/cm**3 catalyst
C-----
      A1 = -XKM1*SA*CA0*CA0*X3
      B1 = X3*CA0*CA0*XKM1*SA*Y(1) - XKM1*SA*CA0 -
1    XKM1*SA*CA0*CA0*X2*(ONE - Y(1)) - X1*CA0
      C1 = XKM1*SA*CA0*Y(1) + XKM1*SA*CA0*CA0*X2*(Y(1) - Y(1)*Y(1))
      XAS = (-B1 - DSQRT(B1*B1 - FOUR*A1*C1))/(TWO*A1)
      IF(XAS.GT.ONE) WRITE(*,15) XAS
      YDOT(1) = - (ONE/VEL)*XKM1*SS*(Y(1) - XAS)
      RETURN
      END

```

```

      SUBROUTINE PEDERV(N,T,Y,PD,N0)
      IMPLICIT REAL*8 (A-H, O-Z)
      DIMENSION Y(N0), PD(N0,N0)
      RETURN
      END

```

C-----
C File MONO1.DAT provides input parameters to run
C Fit parameter routine, MONO1.F
C-----

| | |
|---------------|------------------------------------|
| 52 | NUMBER OF DATA POINTS |
| .46429200E+04 | A0 |
| .46250500E+08 | B0 |
| .33751100E+08 | D0 |
| .60752800E+04 | EA/R |
| .44557700E+04 | EB/R |
| .26948300E+04 | ED/R |
| .10000000E+01 | CATALYST BED DENSITY (G/CM**3) |
| .10000000E-04 | INITIAL STEP SIZE (CM) |
| .50000000E+01 | Catalyst Length, cm (TOUT) |
| .10000000E-05 | ERROR TOLERANCE (EPS) |
| .57315000E+03 | Reference Temperature, K (TREF) |
| .13061000E+01 | PRESSURE (ATM) (PRESS) |
| .10370000E+00 | CELL RADIUS (CM) |
| .35000000E-02 | WASHCOAT THICKNESS |
| .11500000E-01 | SUBSTRATE THICKNESS |
| .77500000E+01 | MASS TRNASFER COEFFICIENT, CM**2/S |
| .50000000E+04 | DELA |
| .50000000E+04 | DELB |
| .50000000E+04 | DELD |
| .10000000E+02 | DEL1 |
| .10000000E+02 | DEL2 |
| .10000000E+02 | DEL3 |

DISTRIBUTION LIST FOR ERDEC-CR-219

| NAMES | COPIES | NAMES | COPIES |
|---------------------------------------|--------|--|--------|
| CDR USA CBDCOM | | | |
| AMSCB CG E4435 UPCHURCH | 1 | COMMANDER | |
| AMSCB CII E3330 LIBRARY | 2 | US ARMY ARMOR CENTER | |
| AMSCB CIH E5183 SMART | 1 | MOUNTED WARFIGHTING BATTLESPACE BATTLE | |
| 5232 FLEMING ROAD | | LABORATORY | |
| ABERDEEN PROVING GROUND MD 21010-5423 | | ATTN ATZK MW | 1 |
| | | FORT KNOX KY 40121-5000 | |
| DIR USA ERDEC | | | |
| SCBRD ASI E5101 FAMINI | 1 | COMMANDER | |
| SCBRD RT E3330 TECH REL OFC | 1 | US ARMY READINESS GROUP | |
| SCBRD RT E3330 J WILLIAMS | 1 | ATTN AFKB RG FS CS | 1 |
| SCBRD RTE E3330 D REED | 25 | FORT SILL OK 73503-6700 | |
| 5232 FLEMING ROAD | | | |
| ABERDEEN PROVING GROUND MD 21010-5423 | | DEFENSE TECHNICAL INFORMATION CENTER | |
| | | 8725 JOHN J KINGMAN ROAD | 12 |
| DIRECTOR | | SUITE 0944 | |
| US ARMY MATERIEL SYSTEMS ANALYSIS | | FT BELVOIR VA 22060-6218 | |
| ACTIVITY | | | |
| ATTN AMXSY CB W HEAPS | 1 | OUSD/DTSA/TD | |
| 392 HOPKINS ROAD | | ATTN PATRICIA SLYGH | 1 |
| ABERDEEN PROVING GROUND MD 21005-5071 | | 400 ARMY NAVY DRIVE ROOM 305 | |
| | | ARLINGTON VA 22202 | |
| COMMANDANT | | | |
| US ARMY INFANTRY SCHOOL | | | |
| ATTN ATSH WC | 1 | | |
| FORT BENNING GA 31905-5400 | | | |